PalZ (2025) 99:285–318
https://doi.org/10.1007/s12542-025-00726-z

RESEARCH PAPER

Diversity of gobioid fishes in the late Middle Miocene of northern Moldova, Eastern Paratethys—part III: dwarf gobies

Bettina Reichenbacher[1,2] · **Alexander F. Bannikov**[3]

Received: 1 October 2024 / Accepted: 23 March 2025 / Published online: 23 June 2025

Abstract

The Middle Miocene (upper Serravallian, Sarmatian sensu latu, Volhynian) deposits at Karpov Yar near Naslavcea, northern Moldova, yield exceptionally preserved fish fossils, often with otoliths in situ. This study, the third in our series on goby fossils from Karpov Yar, describes four new dwarf goby species (standard lengths 16–34 mm), including two new genera: †*Moldavigobius gloriae* sp. nov., †*Cryptograciles conicus* gen. et sp. nov., †*Cryptograciles robustus* gen. et sp. nov., and †*Alienagobius pygmaeus* gen. et sp. nov. A fifth species is left in open nomenclature as †*Moldavigobius* sp. The new genera share 27 vertebrae (10 abdominal), a D1 with six spines, a D2 with a spine and 9–11 rays, and ctenoid flank scales. Differences include the D1-pterygiophore formula, pelvic- and anal fin ray counts, scale number, and otolith morphology. The phylogenetic analyses suggest that †*Moldavigobius* spp. could be part of the *Aphia* lineage (Gobiidae), †*Cryptograciles* gen. nov. may belong to the *Pomatoschistus* lineage (Oxudercidae), and †*Alienagobius* gen. nov. possibly represents a stem member of the *Stenogobius* lineage, although this is surprising given the tropical biogeography of this lineage and its absence in the fossil record. Morphological similarities across the fossil genera likely reflect adaptations to a cryptobenthic lifestyle in a low-energy, lagoonal environment, while variations in scales and otoliths between species indicate microhabitat specialization. Our findings suggest Karpov Yar was an ecologically dynamic site, providing various microhabitats that allowed for the coexistence of multiple cryptobenthic goby species.

Keywords Fish fossils with otoliths in situ · New genus · Eastern Paratethys · Northern Moldova · Serravallian

Introduction

The present study continues our research on well-preserved, articulated skeletons of gobioid fishes (gobies in the following) from the Middle Miocene sediments at the Karpov Yar ravine, in the vicinity of the township Naslavcea, northern Moldova. The age of the sediments is upper Serravallian (ca. 12 Ma) and corresponds to the Sarmatian sensu lato stage and the Volhynian substage, respectively (Reichenbacher and Bannikov 2022, 2023). The Karpov Yar locality, situated in the western sector of the Eastern Paratethys, has long been known for its well-preserved and diverse marine fish fauna and terrestrial flora (Reichenbacher and Bannikov 2022 and references therein). Moreover, it has revealed a surprisingly high diversity of gobies, including several new genera and species. A notable feature of the fish fossils from Karpov Yar is their well-preserved articulated skeletons, often with otoliths preserved in situ.

This study is the third part of our description of the goby assemblage from Karpov Yar. In the first part, we described four new genera and six species that resembled the present-day genus *Lesueurigobius* (so-called '*Lesueurigobius* look-alikes') and interpreted them as stem members of the *Aphia* lineage (sensu Agorreta et al. 2013) of the European Gobiidae. The species included †*Katyagobius prikryli* Reichenbacher & Bannikov, 2022, †*Pseudolesueurigobius manfredi* Reichenbacher & Bannikov, 2022, †*Sarmatigobius compactus* Reichenbacher & Bannikov, 2022, †*S.*

Handling Editor: Jürgen Kriwet.

✉ Bettina Reichenbacher
b.reichenbacher@lmu.de

Alexander F. Bannikov
aban@paleo.ru

[1] Department of Earth and Environmental Sciences, Ludwig-Maximilians-Universität München, Richard-Wagner Straße 10, 80333 Munich, Germany

[2] GeoBio-Center, Ludwig-Maximilians-Universität München, Munich, Germany

[3] Borissiak Paleontological Institute, Russian Academy of Sciences, Profsoyuznaya ul. 123, Moscow 117647, Russia

iugosus (Schwarzhans, Brzobohatý & Radwańska, 2020), †*Yarigobius decoratus* Reichenbacher & Bannikov, 2022, and †*Y. naslavcensis* Reichenbacher & Bannikov, 2022. In the second part, we have introduced a further new genus and species, †*Moldavigobius helenae* Reichenbacher & Bannikov, 2023, characterized by a small body size, large ctenoid scales, and nearly square otoliths (sagittae), which we considered as a possible member of the extant *Aphia* lineage (sensu Agorreta et al. 2013) within the European Gobiidae. The fourth and final part of our study on the goby assemblage from Karpov Yar will focus on fossils representing extinct species of the modern Ponto-Caspian goby group.

The aim of the present third part of our project is to describe four additional new goby species from Karpov Yar, all of remarkably small size. Among these, one represents another species of †*Moldavigobius*, while the other three belong to new extinct genera: †*Cryptograciles* gen. nov., represented by two new species, and †*Alienagobius* gen. nov., with one new species. We employ both comparative morphology and Bayesian inference phylogenetic analyses to explore their possible relationships and provide a brief account of their palaeoenvironmental information.

Geological setting

At the Karpov Yar locality, diatomites and marls with several thin layers containing numerous well-preserved fish fossils (mass-mortality fish layers) are exposed. These fossiliferous strata overlie clays with abundant terrestrial plant remains, which in turn unconformably lie on Upper Cretaceous conglomerates and cherts (Ionko 1954; Yakubovskaya 1955). Above the fossiliferous diatomites and marls, marine sediments containing molluscs indicative of a Volhynian age are present (Roşca 2008). For additional details of the geological profile and previously described fossils (fishes, molluscs), see Reichenbacher and Bannikov (2022).

Materials and methods

Fossil material

The studied material consists of 12 articulated skeletons that all have otoliths in situ except for PIN 5274/58. Four specimens (PIN 5274/46a-b, PIN 5274/58a-b, PIN 5274/67a-b, PIN 5274/68a-b) are represented based on both part (head to the right, indicated with "a") and counterpart (head to the left, indicated with "b"). Note that for specimens PIN 1306/85b, PIN 5274/27a, and PIN 5274/27b, each preserved on a single plate, the suffixes "a" and "b" are used to distinguish different specimens on the same slab. The skeleton-based material is deposited in the Borissiak Paleontological Institute of the Russian Academy of Sciences in Moscow, under the inventory numbers PIN 1306/85b, PIN 5274/27a, PIN 5274/27b, PIN 5274/34, PIN 5274/43, PIN 5274/46a-b, PIN 5274/47, PIN 5274/51, PIN 5274/58a-b, PIN 5274/67a-b, PIN 5274/68a-b, and PIN 5274/70. The otoliths extracted from some specimens are kept in the Bavarian State Collection for Palaeontology and Geology (SNSB-BSPG) in Munich, Germany, under the inventory number SNSB-BSPG 2021 XI.

Comparative material

Morphometric data for 14 extant gobies (10 marine species of *Gobius*, family Gobiidae; three marine and one freshwater species of *Pomatoschistus*, family Oxudercidae) were compiled from the supplementary material provided by Gut et al. (2020). This dataset served as an actualistic comparative basis for assessing morphometric variation within and between species, in order to estimate the degree of difference that can be expected within a species and, conversely, to identify morphometric differences that may indicate the presence of two distinct species. Details of the species and morphometric variables are presented in Table 1, while the raw measurement data can be found in Supplementary Data 1.

Morphological study of the fossil specimens

Imaging. The fossil skeletons and otoliths were examined and photographed under a Leica M165 FC stereomicroscope equipped with a digital camera (Leica DC 200). Otoliths preserved in situ that were solid enough to allow cautious extraction were carefully removed and are stored separately (PIN 5274/27a, right sagitta, lapillus; PIN 5274/27b, right sagitta; PIN 5274/43, left sagitta, lapillus; PIN 5274/46a-b, both sagittae; PIN 5274/47, left sagitta; PIN 5274/51, left sagitta; PIN 5274/67a, left sagitta). Among the extracted otoliths of very small size, the sagitta of specimen PIN 5274/51, the sagitta and associated lapillus of specimen PIN 5274/43, and the lapillus of specimen PIN 5274/27a were imaged using a HITACHI SU 5000 Schottky FE-SEM at the Department of Earth and Environmental Sciences, LMU Munich. In addition, the sagitta preserved in situ in specimen PIN 1306/85b and the lapillus preserved in situ in specimen 5274/67b were SEM imaged using a TESCAN VEGA II at the Borissiak Paleontological Institute of the Russian Academy of Sciences, Moscow, Russia.

Measurements and interpretation. Morphometric measurements were performed based on photographs of the fossil skeletons. The measurements followed Gut et al. (2020) and Reichenbacher and Bannikov (2022, 2023) and included the following distances: head length (from the tip of the snout to the basioccipital), eye length, lower jaw length, body

Table 1 Variation of morphometric variables (minimum and maximum values in % of standard length) between and within extant goby species; variables that varied by at least 5% SL within a species are highlighted by bolditalics

Species, locality (number of individuals), standard length (SL) in mm		SN/D1	SN/D2	SN/A	D2 C	CPL	BD1	D2b	Ab
Gobius auratus Risso, 1810, Selce (9), SL 26.1–41.6	Min	34.8	52.4	57.7	12.4	18.4	16.9	25.9	19.9
	Max	38.2	56.2	59.8	14.6	21.3	18.1	29.4	24.7
	Diff	**3.4**	**3.9**	**2.1**	**2.3**	**2.9**	**1.2**	**3.6**	**4.7**
Gobius bucchichi Steindachner, 1870, Selce (9), SL 44.4–67.3	Min	29.4	49.5	54.1	10.7	16.6	13.9	30.9	22.8
	Max	33.6	52.9	57.5	13.1	19.9	17.1	33.8	26.7
	Diff	**4.2**	**3.4**	**3.4**	**2.3**	**3.3**	**3.3**	**2.9**	**4.0**
Gobius cobitis Pallas, 1814, Montenegro (10), SL 33.4–80.0	Min	33.8	52.8	58.6	11.3	19.2	14.8	26.6	18.4
	Max	36.9	55.7	60.9	15.3	22.0	18.1	29.6	20.8
	Diff	**3.1**	**2.9**	**2.4**	**4.0**	**2.8**	**3.3**	**3.0**	**2.4**
Gobius couchi Miller & El-Tawil, 1974, Krk (4), SL 32.9–44.3	Min	31.7	50.9	55.5	12.0	19.2	16.5	29.7	22.1
	Max	33.2	54.1	58.6	14.6	22.6	21.0	31.0	23.3
	Diff	**1.5**	**3.2**	**3.1**	**2.6**	**3.4**	**4.6**	**1.3**	**1.3**
Gobius geniporus Valenciennes in Cuvier & Valenciennes, 1837, Selce (6), SL 63.6–129.7	Min	33.0	53.2	57.2	10.0	16.1	14.2	28.2	22.1
	Max	36.6	55.2	61.2	13.2	18.1	16.4	31.4	25.3
	Diff	**3.6**	**2.0**	**4.1**	**3.2**	**2.1**	**2.2**	**3.2**	**3.2**
Gobius incognitus Kovačić & Šanda, 2016, Peljesac (9), SL 44.0–79.0	Min	29.6	49.2	52.4	10.1	16.9	15.6	29.5	23.4
	Max	33.8	52.2	58.4	14.3	21.4	19.7	33.8	28.2
	Diff	**4.2**	**3.0**	***6.1***	**4.1**	**4.5**	**4.1**	**4.3**	**4.8**
Gobius niger Linnaeus, 1758, Pilsey Island (7), SL 40.7–59.5	Min	33.1	52.6	56.2	12.9	18.8	15.7	26.4	19.6
	Max	35.6	56.2	59.4	13.9	21.3	18.8	28.4	23.4
	Diff	**2.5**	**3.6**	**3.3**	**1.0**	**2.5**	**3.0**	**2.0**	**3.7**
Gobius paganellus Linnaeus, 1758, Faro (10), SL 46.8–69.2	Min	32.1	52.4	55.6	10.3	19.2	19.5	28.6	20.0
	Max	35.4	55.2	59.4	13.5	22.3	21.6	32.3	24.0
	Diff	**3.2**	**2.8**	**3.8**	**3.2**	**3.1**	**2.2**	**3.7**	**4.0**
Gobius roulei de Buen, 1928, Selce (4), SL 52.0–56.2	Min	33.2	51.2	56.7	12.6	18.6	14.3	28.7	21.5
	Max	36.6	55.8	59.9	13.6	19.6	16.9	31.8	24.6
	Diff	**3.4**	**4.6**	**3.1**	**1.0**	**1.0**	**2.6**	**3.2**	**3.1**
Gobius vittatus Vinciguerra, 1883, Selce (9), SL 17.3–43.2	Min	31.9	51.7	56.7	15.7	20.0	16.5	24.3	17.4
	Max	36.6	56.3	60.4	19.4	24.3	21.4	27.3	22.2
	Diff	**4.7**	**4.6**	**3.7**	**3.7**	**4.3**	***5.0***	**3.0**	**4.8**
Pomatoschistus knerii (Steindachner, 1861), Krk (10), SL 21.6–27.0	Min	35.6	54.9	55.7	21.1	23.4	13.3	15.7	15.0
	Max	38.6	57.7	58.4	24.1	27.6	16.5	19.5	20.3
	Diff	**3.0**	**2.8**	**2.7**	**3.0**	**4.2**	**3.2**	**3.7**	***5.4***
Pomatoschistus marmoratus (Risso, 1810), Selce (7), SL 24.8–37.1	Min	36.2	56.4	56.6	18.8	22.8	14.8	16.2	14.3
	Max	39.9	59.6	62.4	21.5	27.5	18.5	19.9	18.3
	Diff	**3.7**	**3.2**	***5.7***	**2.8**	**4.7**	**3.7**	**3.7**	**4.0**
Ninnigobius montenegrensis (Miller & Šanda, 2008), Skadar Lake (10), SL 17.7–23.7	Min	38.6	56.2	58.7	21.4	25.7	15.7	12.6	10.0
	Max	41.0	59.2	61.8	26.9	30.6	19.4	17.5	13.6
	Diff	**2.4**	**3.0**	**3.2**	***5.5***	**4.9**	**3.7**	**4.9**	**3.5**
Pomatoschistus quagga (Heckel, 1837), Krk (10), SL 26.3–29.9	Min	32.9	53.3	53.5	22.8	27.6	11.3	15.8	13.4
	Max	35.3	55.7	57.4	26.3	30.6	13.4	18.4	16.9
	Diff	**2.4**	**2.4**	**4.0**	**3.5**	**3.0**	**2.0**	**2.6**	**3.5**

Data compiled from Gut et al. (2020). Individual measurements of each specimen are provided in the Supplementary Data 1. For collection numbers of species and geographic coordinates of sites see Gut et al. (2020)

Ab anal-fin base, *BD1* body depth at insertion of D1, *CPL* caudal peduncle length, *D2b* second dorsal-fin base, *D2C* distance between the end of D2 and the first procurrent caudal-fin ray, *SN/A* prenanal distance, *SN/D1* predorsal distance to D1, *SN/D2* predorsal distance to D2

proportions, fin sizes, fin base lengths, distance between D1-spines, and length of the spine in the D2, anal fin, and pelvic fin. Additionally, scale height was measured as the maximum vertical size of the scale. All measurements were recorded to the nearest 0.1 mm using ImageJ (Schneider et al. 2012) and were normalized using either the standard length (SL) or head length (HL) of the fossil as reference.

Because of the limited number of specimens available for each species and the incomplete preservation of some, statistical tests to evaluate the significance of morphological differences between species or genera could not be performed. Instead, for taxonomic purposes, we considered only those body morphometric variables that differed by at least 5% of SL between two taxa as diagnostic of the species or genus. This 5% threshold is based on the observed intraspecific morphometric variation in the comparative dataset (Table 1). When ranges are provided, the 5% threshold applies to the difference between the ranges, specifically the maximum value of a variable in one taxon and the minimum value in the other taxon (or vice versa). For example, caudal peduncle length would be considered different if its range were 15–17% SL in one taxon and 22–25% SL in the other, but not if the range in the second taxon were 21–25%.

Meristic and osteological characters. When preservation quality allowed, counts were conducted for the abdominal vertebrae, caudal vertebrae (including the terminal centrum), fin rays (with every discernible ray counted), and scales in the longitudinal row. If recognizable, the pterygiophore formula of the first dorsal fin (D1) was determined following Birdsong et al. (1988). In specimen PIN 1306/85b, a direct count of scales in the longitudinal row was not possible due to preservation issues. Instead, the horizontal length of two overlapping scales was measured, and the total scale number was estimated based on the standard length of the specimen. Standard terminology for osteological characters followed Reichenbacher and Bannikov (2022, 2023) with topographical terms referring to the natural anatomical location of the described structures.

Otoliths, otolith morphometry, and statistical analysis. The terminology for sagitta and lapillus followed the definitions provided by Reichenbacher and Bannikov (2022, 2023). Sagitta measurements included the sulcus inclination angle (SuA) and seven linear dimensions: maximum otolith length (OL), maximum otolith height (OH), colliculum length (CoL), horizontal sulcus length (SuL), vertical sulcus height (SuH), vertical distance from the sulcus tip to the ventral otolith margin (SuTipV), and vertical distance from the sulcus end to the ventral otolith margin (SuEndV).

The linear measurements were standardised by expressing them as percentages of either OL, OH, or SuEndV as reference values. For LH (length-to-height ratio), the ratio of OL to OH was calculated. Accordingly, the following nine otolith variables were obtained: LH, CoL (%OL), SuL (%OL), SuL (%OH), SuH (%OL), SuH (%OH), SuTipV (%SuEndV), SuTipV (%OH), and SuEndV (%OH). The SuA measurement was treated as a separate variable and used as well (for details see Reichenbacher et al. 2023).

The ten variables were subjected to descriptive statistical analysis using the PAST software (version 4.03; Hammer et al. 2001) to quantitatively assess otolith differences between genera and species. The Shapiro–Wilk test was applied to evaluate the normality of each variable's distribution ($p > 0.05$ indicating normal distribution). Since most variables had a normal distribution, a one-way ANOVA with post-hoc tests was performed to assess differences in otolith variables across multiple groups with differences considered significant at $p < 0.05$. Tukey's post-hoc test was applied when Levene's test indicated homogeneity of variance ($p > 0.05$). If variances were heterogeneous (Levene's test, $p < 0.05$), the Mann–Whitney post-hoc test with Bonferroni-corrected p-values was used. For comparison between two groups, a T-test (with and without Monte Carlo permutation) was conducted for normally distributed variables to detect significant differences ($p < 0.05$). For non-normally distributed data, the Mann–Whitney test was employed ($p < 0.05$).

Phylogenetic analysis

A total-evidence matrix suitable for the phylogenetic analysis of gobioid fossils has recently been made available by Gierl et al. (2022) and Dirnberger et al. (2024). The latest version of this matrix (Dirnberger et al. 2024) includes morphological and molecular data for 48 extant gobioid species, representing each family, as well as data for *Sphaeramia nematoptera* Bleeker, 1856 (Apogonidae), which was used as the outgroup. To this dataset we added the morphological characters of †*Moldavigobius* and the two new genera described here, and examined their phylogenetic placement using Bayesian inference, implemented in MrBayes 3.2.7a (Ronquist et al. 2012) via the CIPRES Science Gateway version 3.3 (Miller et al. 2010). Parameter settings, model selection, and assessment of convergence for the Bayesian inference were performed following Dirnberger et al. (2024). The phylogenetic results were summarized in a 50% majority-rule consensus tree with posterior probabilities (PP) and were rooted and visualized using FigTree 1.4.4 (Rambaut 2018). The input files of the Bayesian analyses are publicly available on Figshare:

https://figshare.com/account/home#/projects/244994

Abbreviations used in the text

For skeletons. BD1, body depth at insertion of D1; BD2, body depth at insertion of anal fin; D1, first dorsal fin; D2, second dorsal fin; D2 C, distance between the end of D2 and the first procurrent caudal-fin ray; HY, hypural; PU, preural vertebra; SL, standard length. Further abbreviations are explained in the captions of the figures and tables. A dagger (†) precedes the name of an extinct genus or species.

For otoliths. CoL, colliculum length; LH, ratio OL-OH; OH, maximum otolith height; OL, maximum otolith length; SuA, sulcus inclination angle; SuH, vertical sulcus height; SuL, horizontal sulcus length; SuEndV, vertical distance from the end of the sulcus to the ventral otolith margin; SuTipV, vertical distance from the tip of the sulcus to the ventral otolith margin.

Institutional abbreviations. PIN, Borissiak Paleontological Institute of the Russian Academy of Sciences, Moscow, Russia; SNSB-BSPG, Bavarian State Collection for Palaeontology and Geology, Munich, Germany.

Systematic palaeontology

The systematic classification and higher clade definitions follow Near and Thacker (2024). The distinction between the families Gobiidae and Oxudercidae is based on Nelson et al. (2016).

Order **Gobiiformes** Bleeker, 1859
Suborder **Gobioidei** Bleeker, 1849
Family **Gobiidae** Cuvier, 1816 sensu Nelson et al. (2016)

Genus †***Moldavigobius*** Reichenbacher & Bannikov, 2023

Type species. †*Moldavigobius helenae* Reichenbacher & Bannikov, 2023

†***Moldavigobius gloriae*** sp. nov.
Figures 1a, 2a, 3

Type material. Holotype, PIN 5274/46a-b, 33.5 mm SL; part (well-preserved) and counterpart (head incomplete, skeleton complete) in lateral view (Fig. 1a, Supplementary Data 2), with left sagitta in situ in the part and right sagitta in the counterpart.

Type locality and age. Karpov Yar ravine, Naslavcea, northern Moldova; upper Serravallian, lower Sarmatian sensu lato (Volhynian).

Referred material. None.

Etymology. The species epithet honours Prof. Dr. Gloria Arratia (University of Kansas, Lawrence, Kansas, USA) for her outstanding contributions to the morphology, osteology, and systematics of both fossil and extant teleost fishes, as well as for her long-term mentorship of the first author's academic career.

LSID ZooBank. This new species is registered under https://zoobank.org/NomenclaturalActs/914C2C75-3BD6-491A-9E8F-7589547F927C.

Generic classification. The new species is assigned to the genus †*Moldavigobius* based on its shared traits with †*M. helenae*, the type species of the genus. These shared characteristics include the main features of the squamation, such as the presence of large, aliform-shaped flank scales, fewer than 30 scales in the longitudinal row, and squarish-to-slightly rectangular sagittae with a narrow sulcus (i.e., a relatively small sulcus height). Additional shared traits include a premaxilla with a distinct postmaxillary process, 10 abdominal and 17 caudal vertebrae, fin formulae for D2 and the anal fin (I, 11 each), the insertion of the anal fin one vertebra behind the origin of D2, an abdominal part of the vertebral column that comprises approximately 66% of the total length of the caudal part, and several other morphometric traits (for details see Table 2 and Supplementary Data 3).

Diagnosis. †*Moldavigobius gloriae* sp. nov. is a small, slender, cylindrical goby with a standard length (SL) of 33.5 mm. The general osteology, morphometry, and meristic traits align with those of the genus, except for specific characters that distinguish it from †*M. helenae*. These differences include a relatively longer lower jaw (47% HL vs. 34–36% HL), a slenderer body (BD1 12.5% SL vs. 17.2–21.0% SL; BD2 12.8% SL vs. 20.7–22.2% SL), the insertion of the D2 and anal fin being one vertebra more posterior, flank scales with more numerous radii (14 vs. 8), and sagittae with well-rounded predorsal and posterodorsal curvatures (vs. slightly angular), absence of a subcaudal iugum, and a slightly greater L/H index (for details see Table 2).

The only other nominal species of †*Moldavigobius* is the otolith-based †*M. suavis* (Schwarzhans, 2014, as *Knipowitschia*). The otoliths of †*M. gloriae* sp. nov. differ from those of †*M. suavis* by having a flat, rounded predorsal curvature (vs. slightly bulging), the presence of a preventral protrusion (vs. absent), a slightly greater L/H index, a significantly longer SuL (%OH), and absence of a subcaudal iugum (see Supplementary Data 4-part 2 for statistical tests of otolith variables between the species of †*Moldavigobius*).

Fig. 1 Holotypes of the four new dwarf goby species from the Volhynian of Karpov Yar, near Naslavcea, northern Moldova. **a** †*Moldavigobius gloriae* sp. nov. with left sagitta preserved in situ (PIN 5274/46a). **b** †*Cryptograciles conicus* gen. et sp. nov. with both sagittae preserved in situ (PIN 5274/70). **c** †*C. robustus* gen. et sp. nov. with both sagittae preserved in situ (PIN 5274/34). **d** †*Alienagobius pygmaeus* gen. et sp. nov. with right sagitta preserved in situ (PIN 5274/68b). Scale bars 5.0 mm

Remarks. The otoliths of †*M. gloriae* sp. nov. show some similarities to the otolith-based species †*Knipowitschia polonica* Schwarzhans, Brzobohatý & Radwańska, 2020, from the lower Langhian (lower Badenian) of Poland, particularly in overall otolith shape and the presence of a slightly protruding preventral projection (Supplementary Data 5). However, they differ from those of †*K. polonica* in having a larger sulcus, as shown by significantly greater values in the otolith variables CoL (%OL), SuH (%OH), SuL (%OL) and SuL (%OH) (Supplementary Data 5).

Fossil skeletal material of *Knipowitschia* is currently unknown, but details of the skeleton and squamation in extant species of *Knipowitschia* are provided in Miller (2004). Among other distinctions, *Knipowitschia* species have a total of 30–34 vertebrae (vs. 27 in †*M. gloriae*) and lack scales on the nape and back up to origin of D2 (vs. present in †*M. gloriae*). These differences confirm that †*M. gloriae* cannot be assigned to the genus *Knipowitschia*.

Otoliths of †*Protobenthophilus strashimirovi* Schwarzhans, Bradić & Bratishko, 2017, which may also be considered as similar to the new species, differ from †*M. gloriae* sp. nov. both in the overall outline and sulcus morphology. According to the original description (see Schwarzhans et al. 2017), their outline is characterized by a short posterodorsal projection (vs. no posterodorsal projection in †*M. gloriae* sp. nov.), a posterior margin with a distinct concavity in the middle (vs. weak concavity), and a predorsal curvature which is below the level of the posterodorsal curvature (vs. at same level). The sulcus of this species is positioned slightly supramedian (vs. median in †*M. gloriae* sp. nov.), ostium and cauda are poorly distinguished (vs. well distinguished), and a crista inferior is absent (vs. present). Additionally, the skeleton of †*Protobenthophilus squamatus* Schwarzhans, Ahnelt, Carnevale & Japundžić, 2017 reveals distinctive differences when compared with †*M. gloriae* sp. nov. including presence of five D1-spines and eight D2-rays (vs. six D1-spines and 11 D2-rays in †*M. gloriae* sp. nov.), a naked predorsal region (vs. covered with scales), and a massive head (vs. slender head) with a head length of 32% SL (vs. 23.6% SL).

General description. †*Moldavigobius gloriae* sp. nov. is a relatively small, slender goby (SL 33.5 mm) with a moderately large head (HL 24% SL), almost cylindrical body outline, and low body depths at origin of D1 (12.5% SL) and anal fin (12.8% SL) (Fig. 1a, Table 2, Supplementary Data 2). Base of D2 slightly longer than D2C (22% SL and 18.8% SL, respectively); caudal peduncle only slightly tapered. Number of vertebrae 27 (10 + 17); D1 with six spines, last spine distant from preceding one (distance is 4.5% SL); D1-pterygiophore formula probably 3–22110; D2 and anal fin each with a spine and 11 segmented rays. Pectoral girdle has well developed, roughly hourglass-shaped radial bones with relatively big interspaces; pectoral fins not preserved. Pelvic fins close together, each with a spine and probably five rays. Caudal fin seems to be slightly fan-shaped (entire length not preserved), with 17 segmented rays (nine rays in the upper lobe). Squamation on the middle and posterior portions of body dense, anterior body portion (beneath the D1) less densely scaled (Fig. 1a). Scales ctenoid, relatively large, of aliform shape; estimated number of scales in longitudinal row < 30. Sagittae of rounded-rectangular shape, slightly longer than high (LH 1.02 and 1.08), without posterodorsal projection (Fig. 2a).

Neurocranium. The neurocranium is preserved in lateral view. The frontal bones are not well preserved but seem to be long and narrow above the orbit and widened posteriorly. The parasphenoid is straight and relatively narrow; details of the vomer are not visible. The ethmoid bones of the neurocranium are fragmented, no details are recognisable. Head scales seem to be absent.

Jaws. The mouth gape is moderately wide; the lower jaw articulation is situated just before the middle of the orbit (Fig. 3a1). The dentary is a robust bone and long (46.8% HL) (Fig. 3a1, a3); the anguloarticular is relatively short and has a relatively deep retroarticular process. Of the maxilla, only the articular head is preserved. Of the premaxilla, a massive articular process and slender ascending process are recognizable, while the postmaxillary process is fragmented and only partially preserved (Fig. 3a3). The dentition of the premaxilla and dentary is multiserial; both bones bear slender, curved, sharp conical teeth of different sizes.

Suspensorium, opercular apparatus, and hyoid arch. The suspensorium bones are mostly not well preserved. The symplectic is a slender rod in its lower portion; the metapterygoid is not recognizable. The quadrate is relatively small and triangular. It has a deep and wide indentation in its posterior portion and a well-developed posterior process. Both the palatine and ectopterygoid are badly damaged and no details are recognizable. There is no endopterygoid. The opercle is relatively large, triangular, and tapered ventrally. Further opercular bones are not recognizable. The ceratohyal and epihyal bones form a relatively slender hyoid bar, but the individual bones are incompletely preserved. Most of the branchiostegal rays are not preserved; their total complement is unknown. The interhyal is not preserved.

Branchial arches. Faint remains of the ceratobranchials and few gill filaments are preserved. The pharyngeal dentition consists of slender, sharp conical teeth of different sizes.

Vertebral column. There are 27 vertebrae, of which 10 are abdominal. The length of the abdominal part of the vertebral

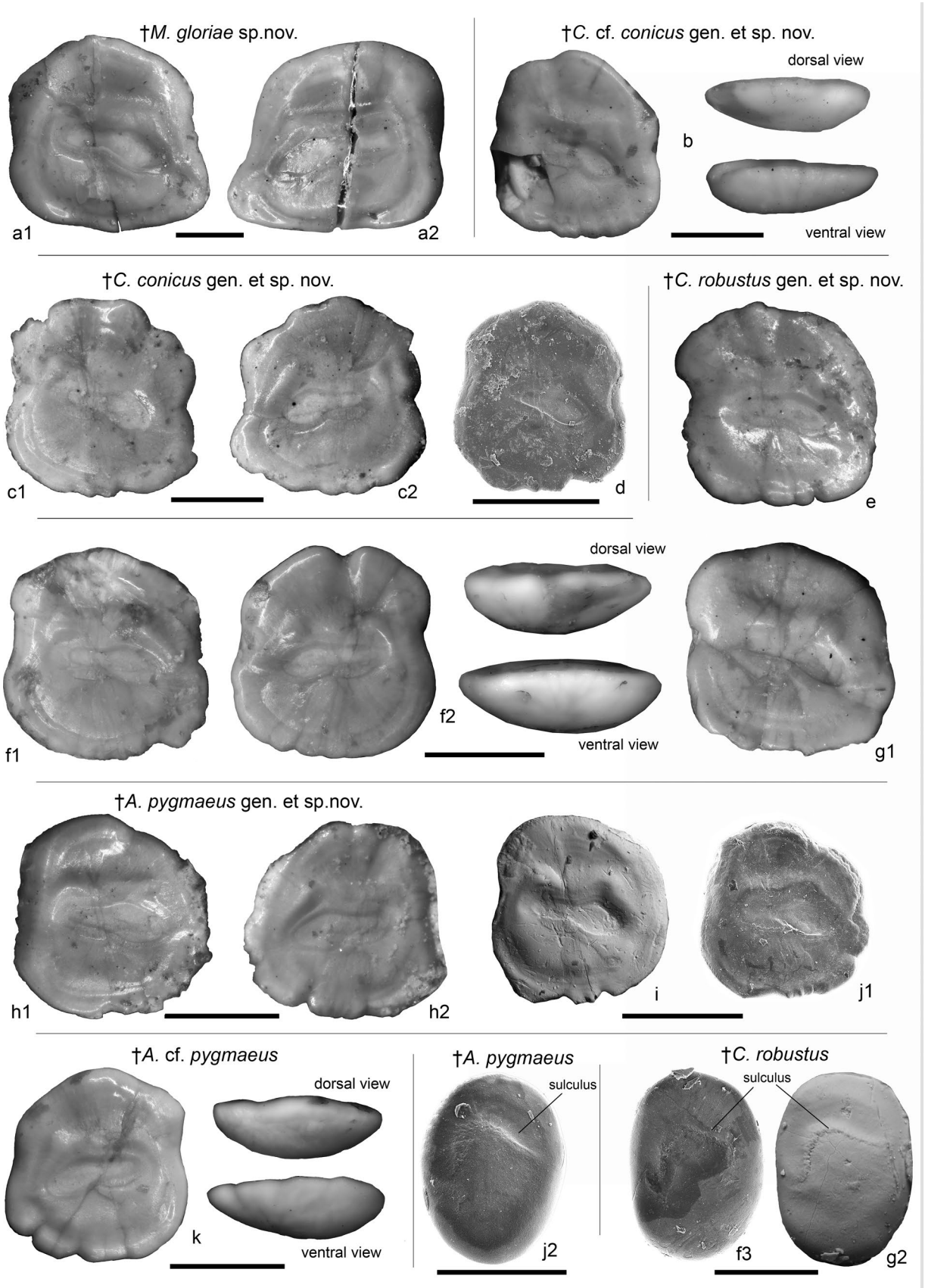
†M. gloriae sp.nov.
a1
a2
†C. cf. conicus gen. et sp. nov.
dorsal view
b
ventral view
†C. conicus gen. et sp. nov.
c1
c2
d
†C. robustus gen. et sp. nov.
e
dorsal view
f1
f2
ventral view
g1
†A. pygmaeus gen. et sp.nov.
h1
h2
i
j1
†A. cf. pygmaeus
dorsal view
k
ventral view
†A. pygmaeus
sulculus
j2
†C. robustus
sulculus
f3
g2

◂**Fig. 2** Otoliths (sagittae, lapilli) found in situ of the studied dwarf gobies from the Volhynian of Karpov Yar, near Naslavcea, northern Moldova. Sagittae are depicted in inner view, if not indicated otherwise; lapilli (**j2, f3, g2**) are shown in ventral view, with the anterior margin at top. **a1**, **a2** Sagitta pair of holotype, PIN 5274/46a-b. **b** Left sagitta, PIN 5274/47a. **c1**, **c2** Sagitta pair of holotype, PIN 5274/70. **d** Left sagitta of paratype, PIN 5274/51. **e** Left sagitta of holotype, PIN 5274/34. **f1–f3** Sagitta pair (**f1**, **f2**) and right lapillus (**f3**) of paratype, PIN 5274/27a. **g1**, **g2** Left sagitta (**g1**) and right lapillus (**g2**) of PIN 5274/67. **h1**, **h2** Sagitta pair of holotype, PIN 5274/68. **i** Left sagitta of paratype, PIN 1306/85b. **j1**, **j2** Left sagitta (**j1**) and right lapillus (**j2**) of paratype, PIN 5274/43. **k** Right sagitta of PIN 5274/27b. Scale bars for sagitta 0.5 mm, for lapilli 0.2 mm

column is 65.6% of the length of the caudal part. Vertebral centra are elongate and distinctively constricted in the middle; the neural spines are short and relatively slender (Fig. 3a2). Parapophyses are visible on the two posterior abdominal vertebrae. The haemal spines are more strongly inclined in the anterior caudal vertebrae than in the subsequent ones. Ribs extend from the third to the last abdominal vertebra; they are strongly inclined and thin; the anterior five rib pairs are relatively long, the subsequent ribs become successively shorter. Few, very tiny epineural bones are visible in the region of the ribs.

Pectoral girdle and fins. The posttemporal is not recognizable. The supracleithrum is elongate and robust, but relatively short; the cleithrum is strong, long and slightly curved (Fig. 3a1). The radial bones of the pectoral fin are relatively large and of more or less hourglass shape (Fig. 3a1). The pectoral fins are not preserved in the holotype, only bases of some of their rays are visible.

Pelvic girdle and fins. The pelvic fins are close together and terminate far from the anal-fin origin (Figs. 1a, 3a1). Their length is 15.2% SL. Each fin consists of a thin, long spine and probably five rays; the rays bifurcate after ca. 30% of their lengths. The basipterygii are relatively slender. The pelvic-fin base is situated under the pectoral-fin base.

Dorsal fins. The first dorsal fin comprises six slender spines; spines I to IV are nearly equally long, spines V and VI are increasingly shorter (Figs. 1a, 3a1). D1-pterygiophore formula is uncertain due to taphonomic distortion of pterygiophores, but seems to be 3–22110 (Fig. 3a1, a2, Supplementary Data 2). The vacant interneural space is located between the neural spines of vertebrae seven and eight.

The origin of D2 is above the junction of vertebrae 11 and 12; the fin consists of a long slender spine and 11 relatively evenly spaced, segmented, distally branched rays (Fig. 1a). The first D2-pterygiophore inserts into the interneural space between the neural spines of the vertebrae eight and nine; the following pterygiophores are strongly inclined (if not displaced post-mortem) and the posterior ones are hardly recognizable (Fig. 3a1, Supplementary Data 2).

Anal fin. The anal fin originates below the junction of vertebrae 12 and 13, i.e., one vertebra behind the D2 origin. It comprises a relatively long spine (6.3% SL) and 11 rays that seem to be more or less equally spaced. Most of the anal-fin pterygiophores are not clearly recognizable.

Caudal endoskeleton and fin. The caudal fin seems to be slightly fan-shaped (Fig. 1a), but its distal part is damaged. There are 17 segmented caudal-fin rays, with nine rays in the upper lobe. Five dorsal procurrent rays and three ventral procurrent rays are visible. Poorly preserved small cycloid scales cover the proximal part of the caudal-fin rays (Fig. 3b1). The caudal skeleton has two relatively large hypural plates (hyp1 +2, hyp3 +4) with a narrow gap in-between; the upper hypural plate is fused with the terminal centrum; hypural 5 is preserved as imprint and seems to be thin and short (Fig. 3b1). The parhypural is rod-like and adjoins both the hypaxial hypural plate and the haemal spine of PU2 (Fig. 3b1). The epural comprises a single large bone with a weak longitudinal ridge along its lower portion (Fig. 3b1). The neural spine of PU2 is poorly preserved; the haemal spine of PU2 is broad and posteriorly expanded; the haemal spine of PU3 is somewhat thicker than that of the preceding vertebra.

Scales. The abdominal portion of the flank is almost scaleless, only some dispersed cycloid scales occur (Figs. 1a, 3a1). The remaining body displays a squamation consisting of large, thick, ctenoid flank scales of aliform shape (Figs. 1a, 3b1, b2). The scales bear up to 14 distinct radii, which have their origin in the posterior portion of the scale from where they spread anteriorly across almost the entire scale (Fig. 3b2). The predorsal region (anterior to and beneath the D1 origin) and the base of the caudal-fin rays are covered with round cycloid scales (Fig. 3a2, b1). Small, rounded, cycloid belly scales are also present.

Otoliths. The holotype part (PIN 5274/46a) is preserved with the left sagitta in situ (Fig. 1a), while the holotype counterpart exposes the right sagitta. Both sagittae possess a rounded-rectangular shape and are slightly longer than high (left sagitta: LH 1.02, right sagitta: LH 1.08) (Fig. 2a1, a2). They have no posterodorsal projection. All margins are smooth; the dorsal and ventral margins are slightly curved, the anterior and posterior margins are slightly concave. There is a notable left–right asymmetry in the preventral curvature, as a preventral projection is clearly present in the right sagitta (Fig. 2a2), but not in the left sagitta (Fig. 2a1). The sulcus is relatively narrow, moderately inclined (16°–17°), and 'shoe-sole' shaped; the cauda is relatively short

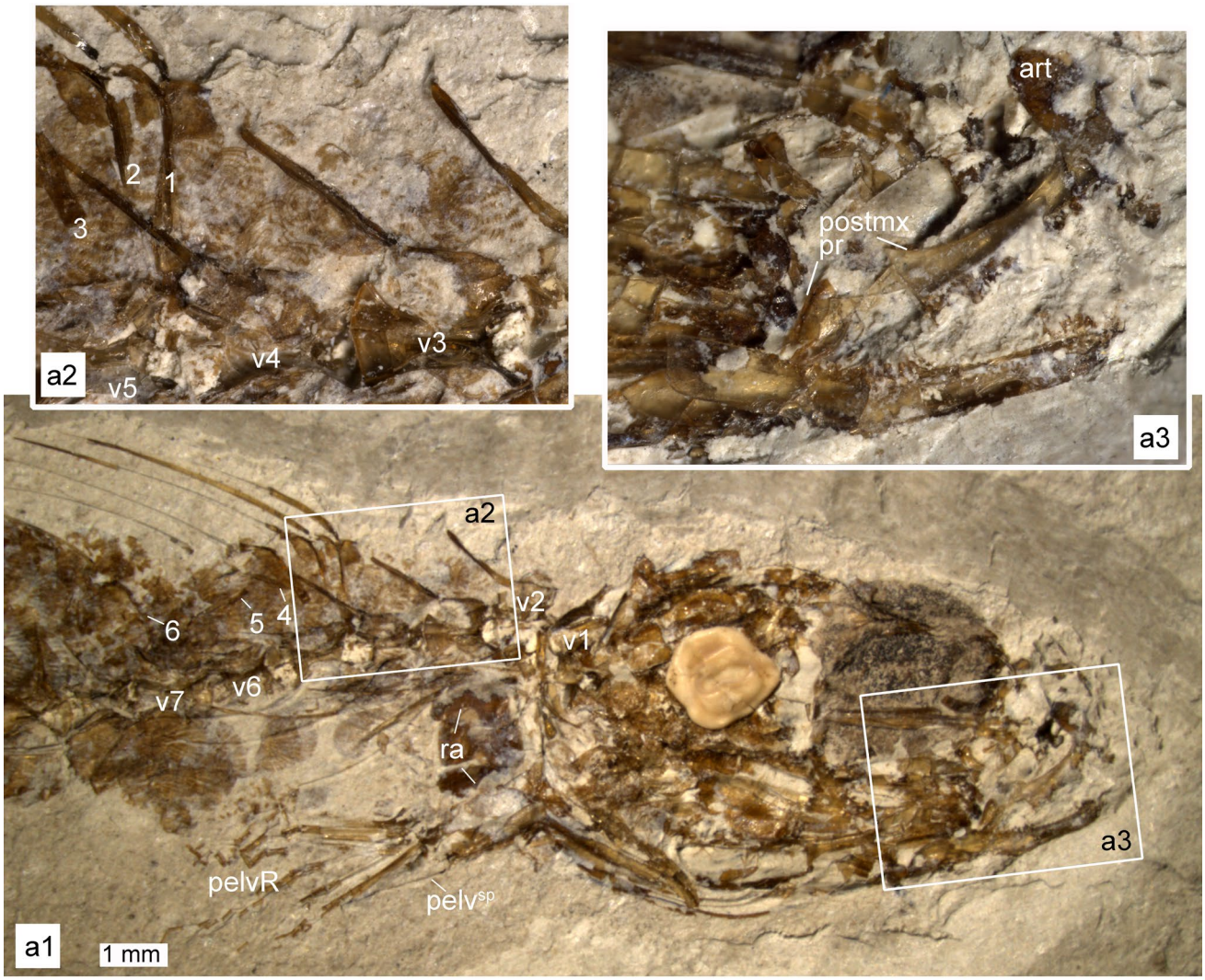
a2
2
1
3
v4
v3
v5
art
postmx
pr
a3
a2
6
5
4
v2
v1
v7
v6
ra
a3
pelvR
pelvsp
a1
1 mm

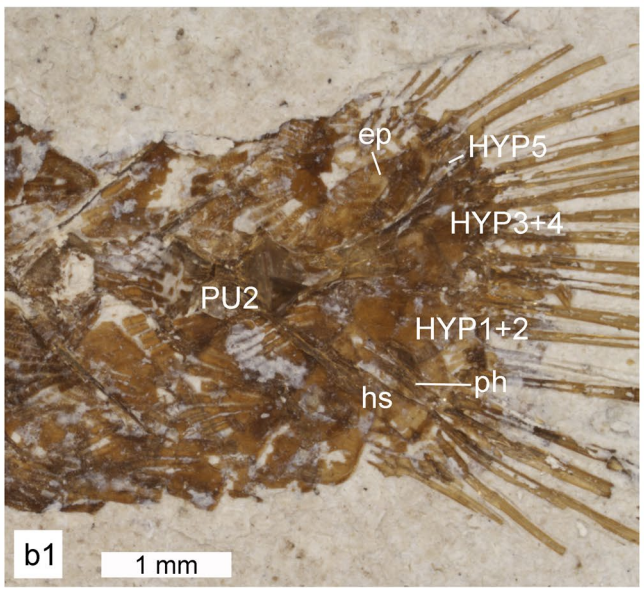
ep
HYP5
HYP3+4
PU2
HYP1+2
hs
ph
b1
1 mm

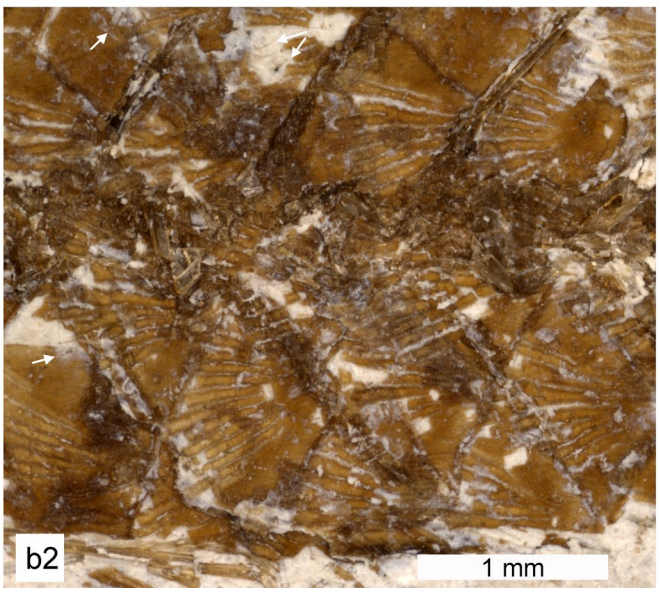
b2
1 mm

◂**Fig. 3** Details of †*Moldavigobius gloriae* sp. nov. from the Volhynian of Karpov Yar, near Naslavcea, northern Moldova. **a** Holotype part (PIN 5274/46a); **a1** head and anterior portion of body with pectoral girdle and partially preserved pelvic fins; **a2** close-up to show predorsal scales and insertion of the first three D1-pterygiophores; **a3** close-up to show well-preserved articular process (art) and partially broken postmaxillary process of the premaxilla. **b** Holotype counterpart (PIN 5274/46b); **b1** posteriormost portion of body and proximal part of caudal-fin rays covered by small cycloid scales; **b2** close-up of flank scales with ctenii partially in situ, partially detached (indicated with arrows). *art* articular process of premaxilla, *ep* epural, *HYP* hypural plate, *hs* haemal spine, *pelvR* pelvic-fin rays, *pelv*^{sp} pelvic fin spine, *ph* parhypural, *postmx pr* postmaxillary process of premaxilla, *PU* preural vertebra, *ra* radials of pectoral girdle, *v* vertebra. Numbers refer to ordinal numbers of D1 pterygiophores and vertebrae, respectively

and posteriorly rounded. A thin, bar-shaped crista inferior extends along the lower sulcus margin, a subcaudal iugum is absent. The ventral line is long; its anterior end is slightly broadened and terminates close to the ostium tip; its posterior end is somewhat indistinct and located approximately opposite to the cauda end. The lapillus is not preserved.

Moldavigobius sp.

Figure 4

Material. Specimen PIN 5274/58a-b, 34.4 mm; part with incomplete and partly disarticulated skeleton (abdominal vertebrae either disarticulated or not preserved, dorsal part of both caudal peduncle and caudal fin lacking) and counterpart (only head and anterior portion of body); part with mold of sagitta preserved in situ.

Locality and age. Karpov Yar ravine, Naslavcea, northern Moldova; upper Serravallian, lower Sarmatian sensu lato (Volhynian).

Remark. With its slender body shape (Fig. 4a1), the presence of robust jaws with a distinct postmaxillary process of the premaxilla and the presence of flank scales with numerous radii (up to 15, Fig. 4a4), the specimen PIN 5274/58 resembles the new species †*M. gloriae* sp. nov. On the other hand, it differs from both †*M. gloriae* sp. nov. and †*M. helenae* in the number of only seven rays in the second dorsal fin and anal fin (vs. 11), in the insertion of the anal fin opposite to the insertion of the second dorsal fin (vs. one vertebra behind), and in the large size of its flank scales (scale height 5.1% of SL, vs. up to 4.2% SL). It is unclear if these differences are owing to the poor preservation of the specimen (it is not perfectly articulated). Further potentially diagnostic characters of specimen PIN 5274/58 are frontal bones that are very narrow above the eyes and markedly widened in the posterior portion (Fig. 4a2) and a triangular opercle that is relatively slender (Fig. 4a3). Frontal bones and opercle shape are unfortunately not well preserved in †*M. helenae* and †*M. gloriae* sp. nov., making comparison impossible. Therefore, specimen PIN 5274/58 is left here in open nomenclature. For details of its morphometric and meristic characters see Supplementary Data 3.

Family **Oxudercidae** Günther, 1861 sensu Nelson et al. (2016)

Genus †***Cryptograciles*** gen. nov.

Type species. †*Cryptograciles conicus* gen. et sp. nov.

Other species. †*C. robustus* gen. et sp. nov. from the same locality.

Etymology. Crypto, from the Greek word *κρυφός* (= hidden), and graciles, modified from the Latin adjective *gracilis* (= slender). The name was selected because a hidden life style can be inferred for this small-sized new taxon. Gender masculine.

LSID ZooBank. This new genus is registered under https://zoobank.org/NomenclaturalActs/FFFE9724-7691-4992-AEB0-F8B0248BA8F1.

Diagnosis. †*Cryptograciles* gen. nov. is a small-sized, moderately slender goby with a standard length (SL) up to 25.5 mm (Fig. 1b, c; Supplementary Data 3 and 6). Head moderately large (24–29% SL), caudal peduncle relatively long (23–25% SL), caudal fin approximately as long as head and slightly fan-shaped. Number of vertebrae 27 (10 + 17), length of abdominal part of vertebral column about 57–65% of that of caudal part. D1 with six spines, last spine distant from preceding one (distance is 3.4–3.5% SL); pterygiophore formula is probably 3–122100. D2 with spine and about 9–11 segmented rays, anal fin with spine and about 9–10 segmented rays, caudal fin with 16–17 segmented rays. Number of pectoral-fin rays is 12–16; pelvic fins separate, each with spine and five rays. Pectoral girdle with four well-developed radial bones of rounded-rectangular shape, with relatively big openings in-between. Dense squamation on body; scales ctenoid, number of scales in longitudinal row 41–44.

Sagitta rounded–squarish (LH 0.89–1.02) with a slightly crenulated ventral margin and no or short posterodorsal projection (Fig. 2b–g1). Sulcus 'shoe-sole' shaped and relatively short, with variable inclination (7.5°–25.0°); cauda usually narrower than ostium. Sulcus with straight or slightly curved crista inferior and flat subcaudal iugum (best visible in the sagittae shown in Fig. 2c and f). Lapillus ovate with clearly defined sulculus (Fig. 2f3, g2).

Table 2 Morphological traits of †*Moldavigobius gloriae* sp. nov., †*M. helenae* Reichenbacher & Bannikov, 2023, †*Cryptograciles* gen. nov. spp. and †*Alienagobius pygmaeus* gen. et sp. nov. from the Volhynian of Karpov Yar (Naslavcea, northern Moldova)

	†***Moldavigobius gloriae*** sp. nov. PIN 5274/46a-b	†***Moldavigobius helenae*** PIN 5274/73, PIN 1306/68b, PIN 1306/68a	†***Cryptograciles*** gen. nov. spp. based on †*C. conicus* gen. et sp. nov. and †*C. robustus* gen. et sp.nov., PIN 5274/70, PIN 5274/51, PIN 5274/47, PIN 5274/34, PIN 5274/27a, PIN 5274/67a-b	†***Alienagobius pygmaeus*** gen. et sp. nov. PIN 1306/85b, PIN 5274/27b, PIN 5274/68a-b, PIN 5274/43
Standard length (SL) in mm	33.5	24.2–34.2	16.8–25.5	c. 16.1–20.1
Morphometric characters in % SL (lengths eye and lower jaw in % HL)				
Head length	23.6	25.8–26.9	23.9–28.7	25.4–27.4
Length eye (% HL)	c. 29.1	21.7–29.3	c. 23.2–28.6	21.2–29.3
Length lower jaw (% HL)	46.8	33.8–35.9	41.5–46.9	41.2
SN/D1	36.4	32.1–36.2	34.6–37.6	36.6–39.0
SN/D2	55.5	49.3–58.2	53.1–55.3	54.6–55.2
D2C	18.8	13.4–18.4	19.5–21.2	14.9
SN/A	58.8	55.4–59.9	56.9–59.0	57.7
CPL	20.3	16.1–17.2	23.4–25.1	23.7–25.9
CPD	8.6	11.1–11.4	6.2–8.7	7.5–9.0
BD1	12.5	17.2–21.0	7.3–16.9	11.2–13.4
BD2	12.8	20.7–22.2	13.7–14.7	11.9–12.4
D1 base	11.6	9.3–10.5	10.2	11.3–11.9
D2 base	22.4	19.8–24.0	19.5–19.6	24.9
Distance insertion D1-spine VI to begin of D2	7.5	6.7–9.1	8.6–8.8	6.0
Distance insertion D1-spine V to VI	4.5	3.8–4.4	3.4–3.5	4.5–c. 5.0
Distance insertion D1-spine IV to V	1.8	1.7–2.3	1.6–1.9	1.7–2.0
Ratio distance D1-spines V–VI to IV–V	2.4	1.7–2.2	1.7–2.2	2.5–2.7
D2 spine length	11.0	8.2–10.3	–	–
Ab	20.9	21.9	15.8–17.6	17.9–c. 19.8
A spine length	6.3	4.1–6.2	–	4.7
A spine length in % of next ray	73	c. 46–60	–	–
Caudal fin length	–	24.3	23.9–27.7	23.4–26.0
Pectoral fin length	–	13.6–16.1	17.4–20.0	–
Pelvic fin length	15.2	14.9–19.3	c. 14.1–16.4	15.9
Pelvic fin spine length	5.1	3.8	–	c. 5.0
Abd. vert. column length	30.7	28.9	27.0–29.9	26.1–26.9
Caudal vert. column length	46.8	43.6	44.6–48.3	46.9–48.7
Abd. vert. column in % of caudal vert. column	65.6	66.4	57.3–64.5	55.1
Meristic and other fin-related characters				
Vertebrae (abd. + caudal)	27 (10 + 17)	27 (10 + 17)	27 (10 + 17)	27 (10 + 17)
D1 spines	VI	VI	VI	VI
D1 pterygiophore formula	Probably 3–22110	Probably 3–22110	Probably 3–122100	3–12…
D2 elements	I, 11	I, 11	I, c. 9, 10–11	I, 10–11
A elements	I, 11	I, 11	I, c. 9, 10	I, 11–12
AP	–	2–?3	2	2

Table 2 (continued)

	†***Moldavigobius gloriae*** sp. nov. PIN 5274/46a-b	†***Moldavigobius helenae*** PIN 5274/73, PIN 1306/68b, PIN 1306/68a	†***Cryptograciles*** gen. nov. spp. based on †*C. conicus* gen. et sp. nov. and †*C. robustus* gen. et sp.nov., PIN 5274/70, PIN 5274/51, PIN 5274/47, PIN 5274/34, PIN 5274/27a, PIN 5274/67a-b	†***Alienagobius pygmaeus*** gen. et sp. nov. PIN 1306/85b, PIN 5274/27b, PIN 5274/68a-b, PIN 5274/43
Segmented caudal fin rays (dorsal/ventral)	9/8	9/8	8–9/7–8	8/7–8
Caudal procurrent rays (dorsal/ventral)	5/min3	(?8) 9/8	7–8/3–6	c. 7/-
Pectoral fin rays	-	c. 15–17	12–16, stiff	14
Pelvic fin elements	I, 5?	I, 5	I, 5 separated	I, 4
Insertion D2 opposite to	v 11/12	v 10, 11	v 11/12–12	v 11–11/12
Insertion A opposite to	v 12/13	v 11	v 12–12/13	v 11–12/13
Caudal fin shape	Slightly fan-shaped	Fan-shaped	Slightly fan-shaped	Slightly fan-shaped
Squamation				
Flank scale type	Ctenoid	Ctenoid	Ctenoid	Cycloid and ctenoid
Radii number	c. 14	8	7–8, weak	6– < 10, thick
Scale height (% SL)	3.9–4.2	3.6–4.8	2.0–2.3	2.6–3.5
Scales in longitudinal row	< 30	< 30	41–44	44
Belly scales	Small, clear circuli	Cycloid, weak radii	Small, round	Cycloid, round
Predorsal scales	Small	Present	Present	Cycloid
Otolith (sagitta) morphometry				
LH	1.02–1.08	0.9–1.03	0.9–1.0	0.9–1.0
CoL (%OL)	50.6–51.3	47.9–53.8	36.5–49.4	42.3–49.4
SuAngle	15.9–16.8	15.7–20.4	7.5–25.1	11.2–15.7
SuL (%OL)	58.5–61.4	58.2–62.2	42.2–51.7	52.9–56.0
SuL (%OH)	59.7–66.5	56.4–59.7	38.7–52.9	51.2–52.8
SuH (%OL)	29.1–34.2	23.5–33.8	18.1–33.7	23.9–26.2
SuH (%OH)	29.7–37.0	24.2–32.5	17.5–34.5	23.0–25.6
SuTipV (%SuEndV)	64.8–65.2	54.7–69.0	57.4–89.5	67.4–78.0
SuTipV (%OH)	30.2–30.3	27.5–33.8	31.0–40.0	33.7–37.8
SuEndV (%OH)	46.5–46.6	47.7–51.0	43.2–54.0	46.1–51.4

For details of specimens see Supplementary Data 2

Abbreviations for skeletons: *A* anal fin, *Ab* anal-fin base, *AP* number of pterygiophores of anal fin inserting before the haemal spine of first caudal vertebra, *BD1* body depth at insertion of D1, *BD2* body depth at insertion of A, *CPD* lowest caudal peduncle depth, *CPL* caudal peduncle length, *D1* first dorsal fin, *D2* second dorsal fin, *D2C* distance between the end of D2 and the first procurrent caudal-fin ray, *HL* head length, *SN/A* preanal distance, *SN/D1* predorsal distance to D1, *SN/D2* predorsal distance to D2, *v* vertebra, vertebrae,—not preserved, *?* not certain due to preservation issues

Abbreviations for otoliths: *CoL* colliculum length, *LH* ratio OL-OH, *SuA* sulcus inclination angle**,** *SuH* vertical sulcus height, *SuL* horizontal sulcus length, *SuEndV* vertical distance from the end of the sulcus to the ventral otolith margin, *SuTipV* vertical distance from the tip of the sulcus to the ventral otolith margin

Differential diagnosis. †*Cryptograciles* gen. nov. differs from †*Moldavigobius* in the D1-pterygiophore -formula (3–122100 vs. 3–22110 in †*Moldavigobius*), presence of two interneural gaps before the insertion of the first D2-pterygiophore (vs. one), and smaller number of anal-fin rays (9–10 vs. 11) (Table 2). Additional differences are apparent regarding squamation and otoliths: The number of flank scales in the longitudinal row is 41–44 (vs. < 30), and the scales are smaller (scale height 2.0–2.3% SL vs. 3.6–4.8% SL) (Table 2). The otoliths have a rounded-to-squarish shape (vs. rectangular), a slightly crenulated ventral margin (vs. smooth), and seven otolith variables are significantly different between the two genera (Supplementary Data 4-part 1).

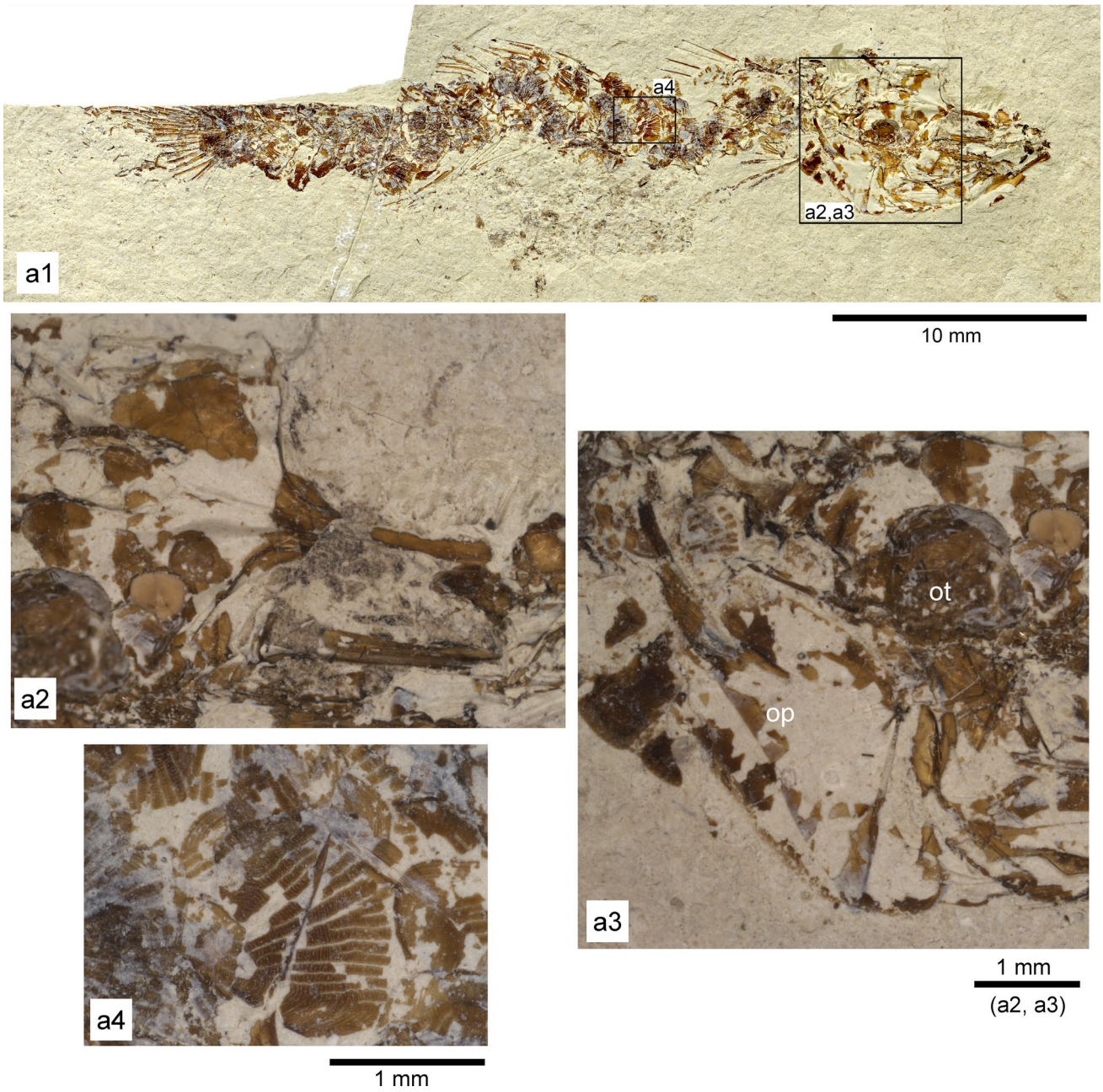

Fig. 4 Details of †*Moldavigobius* sp. from the Volhynian of Karpov Yar, near Naslavcea, northern Moldova (specimen PIN 5274/58a). **a1** Overview of specimen; **a2** close-up of frontal bones; **a3** close-up of opercle (op) and mould of sagitta (ot); **a4** close-up of flank scale below origin of D2

From the '*Lesueurigobius* look-alikes', with which †*Cryptograciles* gen. nov. co-occurs at Karpov Yar (see Reichenbacher and Bannikov 2022), the new taxon can be distinguished by its slightly fan-shaped caudal fin (vs. longish-lanceolate), fewer rays both in the D2 (9–11 vs. 14–16) and anal fin (9–10 vs. 13–15), a different D1-pterygiophore formula (3–122100 vs. 3–22110), and presence of rounded to squarish otoliths possessing a slightly crenulated ventral margin. From other previously described skeletal- and otolith-based marine and brackish fossil goby genera from the western Mediterranean and Paratethyan regions †*Cryptograciles* gen. nov. can be separated by its specific combination of body morphometric, meristic, and otolith characters (Gierl and Reichenbacher 2015; Schwarzhans et al. 2017, 2020a, b, 2022; Carolin et al. 2023; Dirnberger et al. 2024; Schwarzhans et al. 2024).

Remarks. The two species of †*Cryptogracilis* gen. nov. are not optimally preserved and some details are only visible in one specimen, while other details are only visible in the other (Figs. 5, 6, 7; Supplementary Data 3 and 6). Nevertheless, the general osteology and morphometric proportions of the two species appear to be very similar. Therefore, we provide a summary description of the new genus below. Differences between the species relate to the relative length of the abdominal vertebral column, the numbers of rays in the D2 and pectoral fin (Supplementary Data 3), the shape of the frontal bone and the opercle (Fig. 6), the overall otolith morphology (Fig. 2c, d vs. e–g), and the sulcus length (Supplementary Data 4-part 3). See species diagnoses below for details.

***Description of* †*Cryptogracilis* gen. nov.**

Neurocranium. The neurocranium is preserved either in lateral or dorsolateral view. The frontal bones are long, narrow above the orbit and broad posteriorly (Figs. 5a1, 6). The parasphenoid is straight, relatively narrow anteriorly and broadened posteriorly; the vomer is rounded anteriorly. Rounded sphenotic bones and a relatively short ethmoid region are visible in †*C. robustus* gen. et sp. nov. (Fig. 6b), other details of the neurocranium are not recognizable. Head scales seem to be absent.

Suspensorium, opercular apparatus, and hyoid arch. The symplectic is a robust rod in its lower portion; only remains of the metapterygoid are preserved. The quadrate is a roughly triangular bone with a deep and wide indentation in its posterior portion and a strong, thick and pointed posterior process (Fig. 7a1). The ectopterygoid is a relatively long bone, almost straight and tapered anteriorly. There seems to be no endopterygoid. The palatine is T-shaped; its proximal portion is not preserved. The preopercle is slightly curved and crescent-shaped. The opercle is triangular and tapered ventrally; the subopercle is slender (Fig. 6). The interopercle is not visible. The hyoid bar (ceratohyal + epihyal) is relatively straight (Fig. 7a1); the anterior portion of the ceratohyal is slightly broadened, the posterior portion of the ceratohyal is not well recognizable, and the epihyal is triangular. The interhyal is not recognizable. The number of branchiostegal rays seems to be five.

Jaws. The mouth gape is moderately wide; the length of the lower jaw is 42–47% HL. The lower jaw articulation is situated approximately opposite to the posterior third of the orbit (Fig. 7a1). The dentary is slender and long; the anguloarticular is low at the retroarticular process. The maxilla is slender and elongate, slightly broader posteriorly and somewhat bent anteriorly. The premaxilla is moderately long and slightly curved; it has a thin ascending process, a relatively massive, rounded articular process and a moderately developed postmaxillary process (Fig. 7a2). The dentition of the premaxilla is multiserial; the teeth are long, slender, curved and of different sizes.

Branchial arches. Remains of few gill arches (ceratobranchials) are preserved in †*C. robustus* gen. et sp. nov. (Fig. 7a1), and some gill rakers are recognizable in †*C. conicus* gen. et sp. nov. (PIN 5274/70). The pharyngeal dentition includes both thick and slender conical teeth, and the teeth (even the slender ones) are more massive than the oral teeth.

Vertebral column. There are 27 vertebrae, of which 10 are abdominal. The length of the abdominal part of the vertebral column is 57–65% of the length of the caudal part. Vertebral centra in the abdominal part of the vertebral column are elongate and distinctively constricted in the middle (Fig. 7a3), vertebral centra in the caudal part of the vertebral column are also constricted in the middle but seem to be slightly more robust (Fig. 7a4). Parapophyses are visible at the last four abdominal vertebrae (Fig. 5a3, a5) and increase in length posteriorly in the series. The haemal spine of the first caudal vertebra is somewhat shorter than the subsequent ones, which are more or less equally inclined (Fig. 5a5). Ribs are slender and relatively long and extend from the third to the last abdominal vertebra. Few very tiny epineural bones are visible in the region of the ribs.

Pectoral girdle and fins. The posttemporal comprises a flat main body and two processes, of which the anterior one is almost as long as the supracleithrum. The cleithrum is strong, long, and clearly curved; its dorsal tip presents the 'cleithral notch' that is typical for gobioids (see Winterbottom 1993) (Fig. 7a1). The pectoral girdle comprises four well-developed radial bones of rounded-rectangular shape, with relatively big openings in-between (Fig. 5a2). The pectoral fin is well preserved in both †*C. conicus* gen. et sp. nov. (Figs. 1b; 5a1, a2) and †*C. robustus* gen. et sp. nov. (PIN 5274/27a, Supplementary Data 6) and elongate and slightly tapered at its end. The complete number of the pectoral fin-rays is only detectable in †*C. conicus* gen. et sp. nov., in which it is 16 (Fig. 5a2). The pectoral fin-rays are branched at the very end, which gives the fin a "stiff" appearance (Figs. 1b; 5a1, a2; Supplementary Data 6). The pectoral fin length is 17–20% SL.

Pelvic girdle and fins. The pelvic fins are separated by a relatively large gap suggesting that they were separate (clearly visible in the holotype of †*C. conicus* gen. et sp. nov., see Fig. 1b and Supplementary Data 2). Each fin has a slender and moderately long spine and five slender rays. Pelvic-fin length is ca. 14–16% SL, and the fins terminate relatively far from the anal-fin origin. The basipterygii are not well

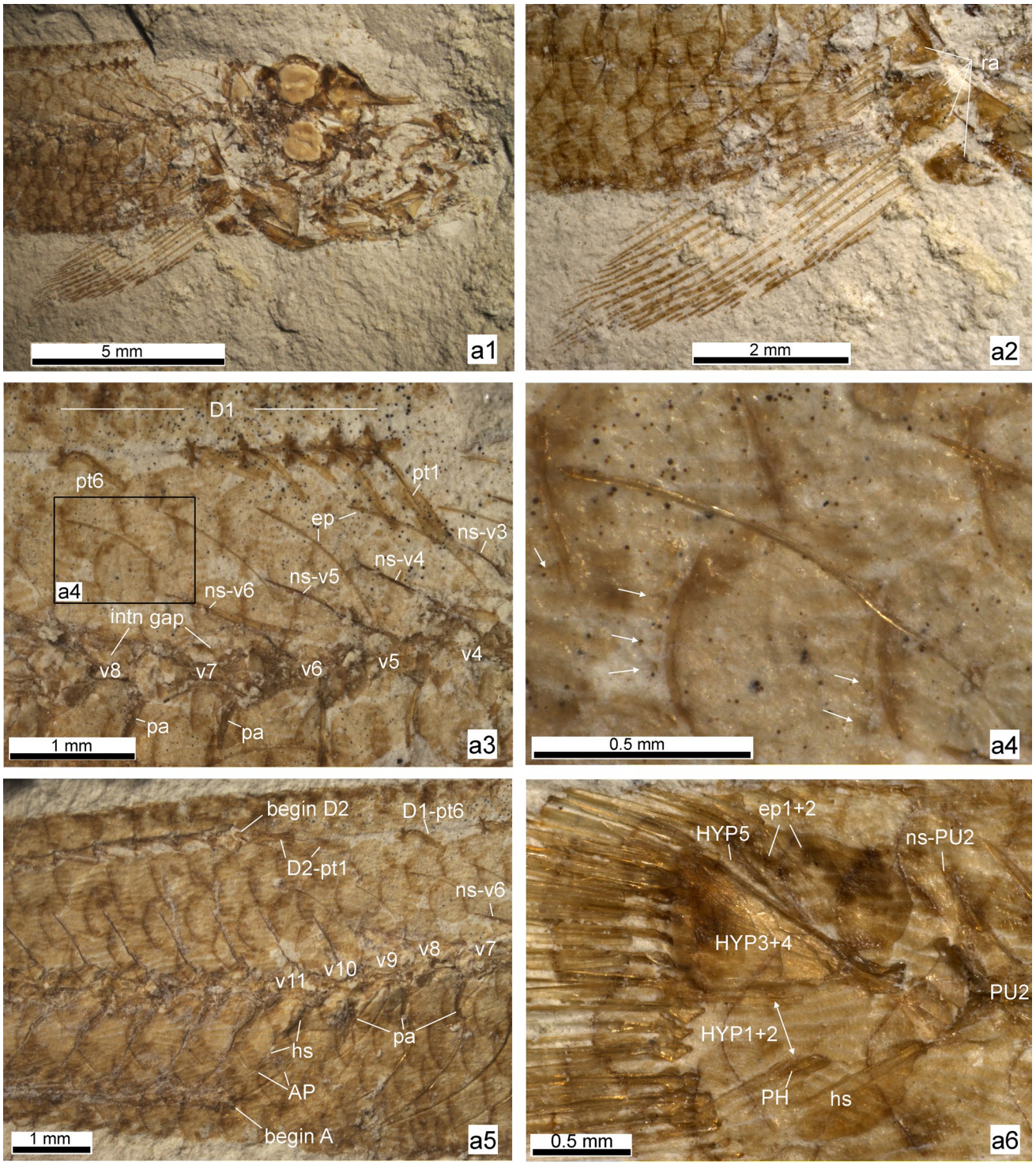

Fig. 5 Details of †*Cryptograciles conicus* gen. et sp. nov. from the Volhynian of Karpov Yar, near Naslavcea, northern Moldova based on the holotype (PIN 5274/70). **a1** Overview of skull (with both sagittae preserved in situ), pectoral girdle, anterior body, and first dorsal fin remains; **a2** close-up of pectoral girdle and fin; **a3** close-up of anterior part of vertebral column, box indicates position of scales shown in a4; **a4** close-up of flank scales below end of D1, arrows indicate ctenii; **a5** close-up of middle part of body showing origin of the second dorsal and anal fins, the first caudal vertebra (v11) and the parapophyses of the last abdominal vertebrae; **a6** caudal skeleton. *A* anal fin, *AP* anal fin pterygiophores inserting before the haemal spine of the first caudal vertebra, *D1* first dorsal fin, *D2* second dorsal fin, *ep* epineural, *hs* haemal spine, *HYP* hypural plate, *intn gap* interneural gap, *ns* neural spine, *pa* parapophysis, *PH* parhypural, *pt* pterygiophores of D1 and D2, *PU* preural vertebra, *ra* radials of pectoral girdle, *v* vertebra (numbers refer to ordinal numbers of vertebrae and D1 pterygiophores, respectively)

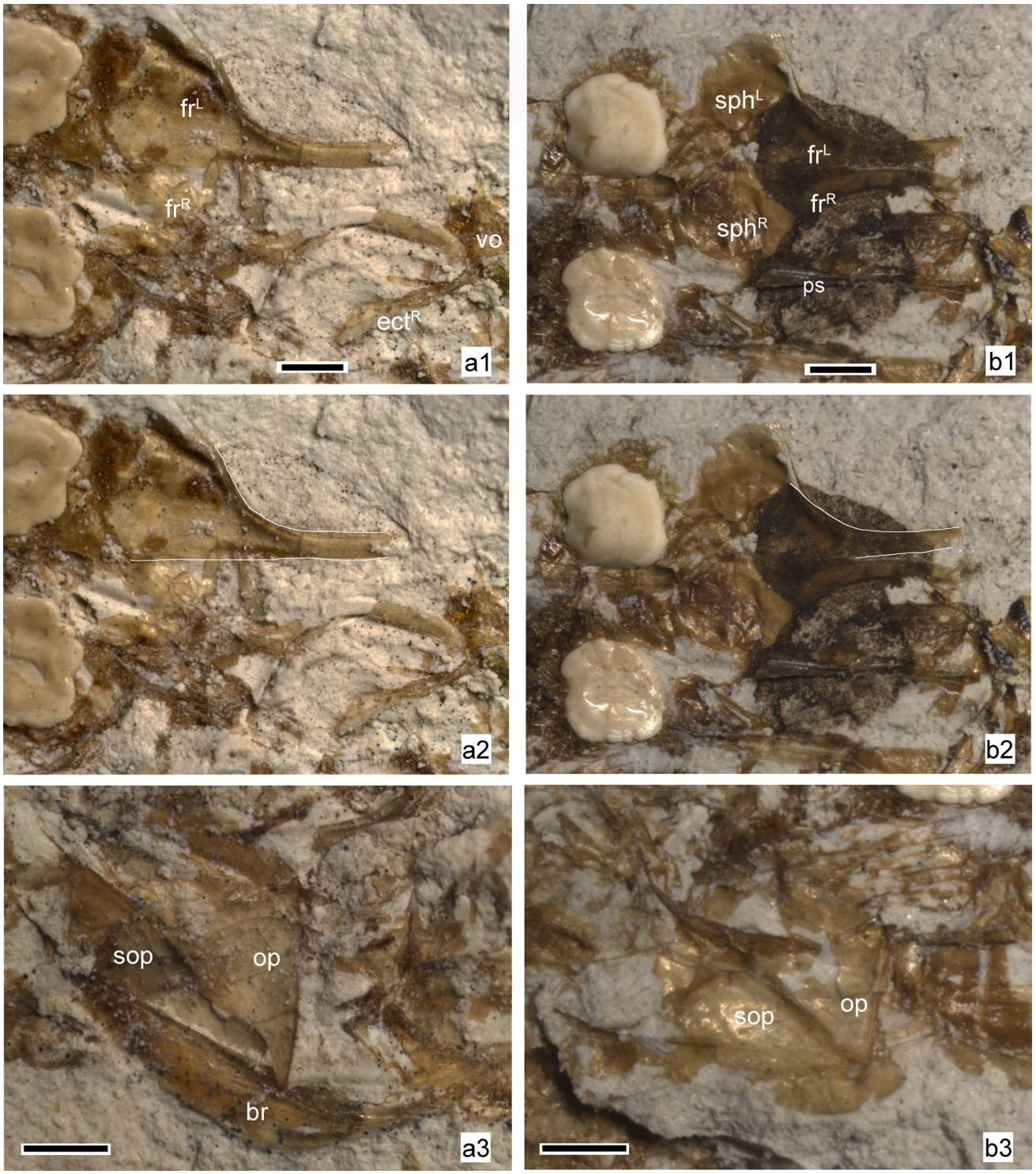

Fig. 6 Differences in the shape of the frontal bone and the opercle between †*Cryptograciles conicus* gen. et sp. nov. (PIN 5274/70) (**a1–a3**) and †*C. robustus* gen. et sp. nov. (PIN 5274/34) (**b1–b3**). Superscripts L and R indicate element from left and right body sides. *br*, branchiostegal ray; *ect*, ectopterygoid; *fr*, frontal bone; *op*, opercle; *sop*, subopercle; *ps*, parasphenoid; *sph*, sphenotic; *vo*, vomer. Scale bars 0.5 mm

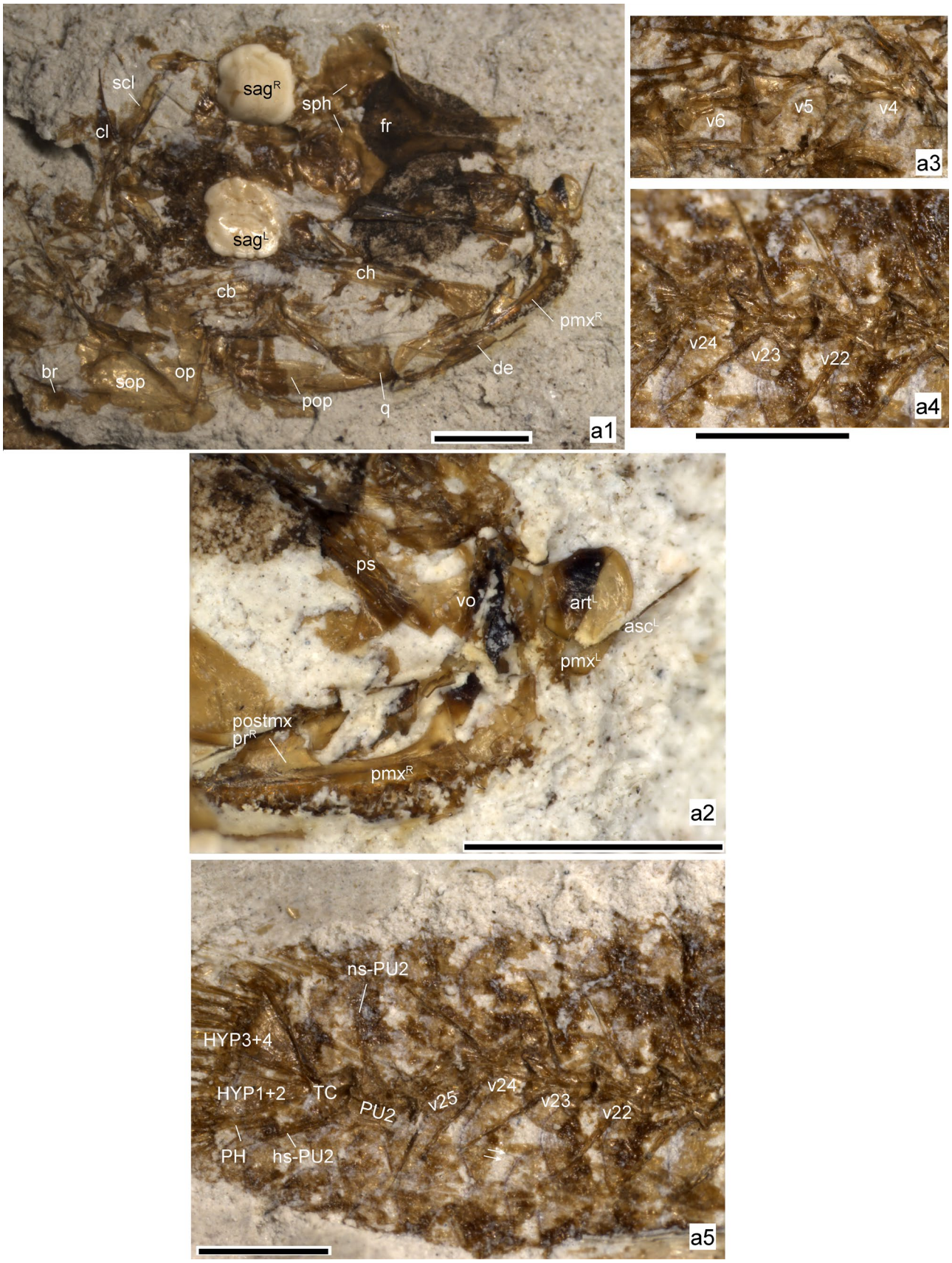
scl
sag^R
sph
cl
fr
sag^L
ch
cb
pmx^R
br
sop
op
pop
q
de
a1
v6
v5
v4
a3
v24
v23
v22
a4
ps
vo
art^L
asc^L
pmx^L
postmx
pr^R
pmx^R
a2
ns-PU2
HYP3+4
HYP1+2
TC
PU2
v25
v24
v23
v22
PH
hs-PU2
a5

◂**Fig. 7** Details of †*Cryptograciles robustus* gen. et sp. nov. from the Volhynian of Karpov Yar, near Naslavcea, northern Moldova based on the holotype (PIN 5274/34). **a1** Overview of skull (with both sagittae preserved in situ) and anteriormost body; **a2** close-up of snout region shown in a1; **a3** three abdominal vertebrae; **a4** three caudal vertebrae; **a5** posteriormost body and caudal skeleton, arrows indicate ctenii. *art* articular process of premaxilla, *asc* ascending process of premaxilla, *br* branchiostegal ray, *cb* ceratobranchial bones, *cl* cleithrum, *ch* anterior ceratohyal (displaced), *de* dentary, *fr* frontal bone, *hs* haemal spine, *HYP* hypural plate, *ns* neural spine, *op* opercle, *PH* parhypural, *pop* preopercle, *postmx pr* postmaxillary process of premaxilla, *pmx* premaxilla, *ps* parasphenoid, *PU* preural vertebra, *q* quadrate, *sag* sagitta, *scl* supracleithrum, *sop* subopercle, *sph* sphenotic, *TC* terminal centrum, *vo* vomer, *v* vertebra (numbers refer to ordinal numbers of vertebrae). Scale bars 1 mm

preserved and seem to be elongate to rounded-triangular in shape.

Dorsal fins. The first dorsal fin contains six spines; the spines are not well preserved in any of the specimens, the last spine being shortest and clearly distant from the preceding one (1.7–2.2x the distance between spines IV and V; Table 2, Supplementary Data 3). The D1-pterygiophore formula seems to be 3–122100 (based on specimen PIN 5274/67, †*Cryptograciles robustus* gen. et sp. nov.); the presence of two interneural gaps between the last D1-pterygiophore and the first D2-pterygiophore is additionally shown by specimen PIN 5274/70 (†*C. conicus* gen. et sp. nov.) (note that the precise formula cannot be identified in this specimen, since the position of the neural spines is disturbed, see Fig. 5a3).

The D2 originates opposite or slightly anterior to the origin of the anal fin, approximately above the second caudal vertebra (Fig. 5a5). It consists of one spine and ca. 9–11 segmented rays; further details of its structure and whether the D2 rays reach the procurrent caudal-fin rays cannot be recognized due to the poor preservation.

Anal fin. The anal fin originates opposite or slightly behind to the D2 origin (Fig. 5a5). It comprises a short spine and ca. 9–10 rays, which are not completely preserved posteriorly. Two anal-fin pterygiophores insert before the haemal spine of the first caudal vertebra (Fig. 5a5).

Caudal endoskeleton and fin. The caudal fin is moderately long (24–28% of SL) and slightly fan-shaped (Fig. 1b, c; Supplementary Data 6). The number of segmented and branched caudal-fin rays is 16–17, with 8–9 rays in the upper lobe and 7–8 rays in the lower lobe. Seven or eight dorsal and three to six ventral procurrent rays are visible. The caudal skeleton has two relatively large hypural plates (HY1 + 2 and HY3 + 4), of which the upper one is fused with the terminal centrum; hypural 5 seems to be relatively short and slim (Fig. 5a6). The parhypural is slender; its entire length is not clear, since the proximal part appears not to be preserved (Fig. 5a6). Two straight, plank-like epurals are present (Fig. 5a6). The penultimate vertebra (preural vertebra 2, PU2) displays an expanded haemal spine and a neural spine that is slightly wider and a little bit shorter than the neural spines of the preceding vertebrae (Figs. 5a6, 7a5). The hypural plates, parhypural, epurals, and the ventral portion around PU2 are covered by a few relatively large ctenoid scales, whereas the proximal portion of the principal caudal-fin rays is covered by two rows of relatively smaller scales (Figs. 5a6, 7a5).

Scales. The body displays a dense squamation consisting of relatively large, ctenoid scales (Figs. 1b, c; 5a5), with 41–44 scales in the longitudinal row. The scales bear about 7–8 radii, their posterior margin is somewhat thickened and has small ctenii (Fig. 5a3, a4). Relatively small cycloid scales cover the belly, the predorsal area, and the base of the caudal-fin rays.

Otoliths. The sagitta is rounded–squarish with a slightly crenulated ventral margin and a wavy dorsal margin (Fig. 2b–g1). The mean L/H index is 0.96 ± 0.04. The sulcus is 'shoe-sole' shaped and relatively short; the sulcus inclination is quite variable (mean value 15.5 ± 6.4). The cauda is narrower than the ostium. The sulcus is adjoined by a straight or slightly curved crista inferior and a flat subcaudal iugum. Based on †*C. robustus* gen. et sp. nov., the lapillus is almost ovate with a straight lateral margin and a slightly curved medial margin. Furthermore, the lapillus presents a well-defined sulculus, which is slightly longer and steeper inclined on the lateral side than on the medial side (Fig. 2f3, g2). For details of otolith measurements see Supplementary Data 3.

†***Cryptograciles conicus*** gen. et sp. nov.
Figures 1b, 2b–d, 5, 6a
Type material. Holotype, PIN 5274/70, 25.5 mm SL; single plate with almost complete skeleton in lateral to slightly dorsolateral view with both sagittae preserved in situ (Fig. 1b). Single paratype is PIN 5274/51a-b (part and counterpart) (Supplementary Data 6).

Referred material. Specimen PIN 5274/47a-b (part and counterpart) (Supplementary Data 6).

This poorly preserved specimen is tentatively assigned as †*C.* cf. *conicus* gen. et sp. nov. based on its otolith morphology (Fig. 2b) and the same relative length of the abdominal part of the vertebral column as in the holotype (57.3% of the caudal part vs. 57.5% in the holotype).

Type locality and age. Karpov Yar ravine, Naslavcea, northern Moldova; upper Serravallian, lower Sarmatian sensu lato (Volhynian).

Etymology. From the Latin adjective *conicus* (= cone-shaped), which refers to the conical body outline of this species.

LSID ZooBank. This new species is registered under https://zoobank.org/NomenclaturalActs/B59D9BA8-1D1B-450B-8864-E0CEE10D4F20.

Diagnosis. †*Cryptograciles conicus* gen. et sp. nov. is a small-sized goby with a conical body outline and a standard length (SL) up to 25.5 mm. The general osteology and morphometry of this species are as described for the genus. The new species differs from its congener †*C. robustus* gen. et sp. nov. in the following traits: calyx-shaped frontal bones that are expanded posteriorly (vs. funnel-shaped and not expanded) (Fig. 6a2 vs. b2), opercle with slightly steeper and slightly more convex anterior margin (Fig. 6a3 vs. b3), slightly shorter lower jaw (41.5% HL vs. 45–47% HL), shorter abdominal part of vertebral column (57.3–57.5% of caudal part of vertebral column vs. 63.2–64.5%), one more D2 ray (11 vs. 10), more pectoral-fin rays (16 vs. ca. 12) (Supplementary Data 3), otoliths without posterodorsal projection (vs. presence of small posterodorsal projection) (Fig. 2b–d vs. 2e–g1), and significantly smaller values in the otolith variables SuL (%OL) and SuL (%OH) (Supplementary Data 4-part 3).

Short description. Small goby up to 25.5 mm SL with a cone-shaped body outline (Fig. 1b, Supplementary Data 2 and 6). Number of vertebrae 27 (10 + 17); D1 with six spines, last spine distant from preceding one; D2 with a spine and 11 segmented rays; number of rays in the anal fin not recognizable. Pectoral fin with 16 rays; pelvic fin with a spine and five rays. Pelvic fins separated by relatively large gap suggesting that they were separate. Caudal fin slightly fan-shaped and about as long as head, with 16–17 segmented rays; 8–9 rays in the upper lobe. For further details see diagnoses for genus and species and Supplementary Data 3.

Otoliths. The sagitta has a squarish to slightly rounded shape, the mean L/H index is 0.94 ± 0.05. The dorsal margin is curved and wavy with a predorsal and posterodorsal corner but no posterodorsal projection (Fig. 2b–d); the predorsal corner is positioned slightly lower than the posterodorsal one. The anterior and posterior margins are relatively smooth and slightly to clearly incised. The preventral transition is rounded or faintly protruding, the posteroventral transition is rounded or has a slight edge. The ventral margin is slightly crenulated and moderately curved. The sulcus is 'shoe-sole' shaped and short, as is characteristic for the genus (see generic diagnosis), but shorter than in †*C. robustus* gen. et sp. nov. A flat subcaudal iugum is present. The sulcus inclination angle ranges between 13° and 25°. The dorsal depression is relatively shallow and the ventral line is clearly incised. No lapilli are preserved. For details of otolith measurements and otolith variables see Supplementary Data 3 and 4.

†***Cryptograciles robustus*** gen. et sp. nov.
Figures 1c, 2e–g, 6b, 7
Type material. Holotype, PIN 5274/34, SL ca. 18.4 mm; single plate with almost complete skeleton preserved in dorsolateral view, with both sagittae in situ (Fig. 1b). Single paratype is PIN 5274/27a (single plate), which is an almost complete skeleton preserved in lateral view, with both sagittae and the right lapillus in situ (Supplementary Data 6).

Referred material. Specimen PIN 5274/67a-b (part and counterpart, Supplementary Data 6), moderately well-preserved specimen with both sagittae and a single lapillus preserved in situ (only the left sagitta could be extracted). It shares with the type specimens of †*C. robustus* gen. et sp. nov. two species-diagnostic morphometric characters (relative lengths of the lower jaw and abdominal part of the vertebral column, Supplementary Data 3), a sagitta with a small, rounded posterodorsal projection, as typical for this species (Fig. 2g1), and the shape of the lapillus (Fig. 2g2). It differs in the presence of a slightly larger and wider sulcus as usually typical for †*Cryptograciles* gen. nov.

Type locality and age. Karpov Yar ravine, Naslavcea, northern Moldova; upper Serravallian, lower Sarmatian sensu lato (Volhynian).

Etymology. From the Latin adjective *robustus*, which refers to the comparatively robust body of this small species.

LSID ZooBank. This new species is registered under https://zoobank.org/NomenclaturalActs/1B535D7D-705D-4F23-9B8F-770C0CE8850C.

Diagnosis. †*Cryptograciles robustus* gen. et sp. nov. is a small-sized goby with a relatively robust body outline; its standard length (SL) reaches 18.4–20.5 mm. The general osteology and morphometry of this species are as described for the genus. For differences from †*C. conicus* gen. et sp. nov. see the diagnosis of the latter.

Short description. Small goby up to 20.5 mm SL with a robust, only slightly tapering body outline (Fig. 1c, Supplementary Data 2 and 6). Number of vertebrae 27 (10 + 17); D1 with six spines, last spine distant from preceding one

(3.4% SL); D2 and anal fin each with a spine and about 9–10 segmented rays. Pectoral fin with 12 rays; pelvic fin with a spine and five rays; pelvic fins seem to be separated. Caudal fin slightly fan-shaped and about as long as head, with 17 segmented rays (8–9 rays in the upper lobe). For further details see Supplementary Data 3.

Otoliths. The sagitta has a squarish to slightly rounded shape (Fig. 2e–g1), the mean L/H index is 0.98 ± 0.03. The dorsal margin is curved, while its precise contour is variable and can bear a relatively deep notch (right sagitta of paratype, Fig. 2f2) or can be almost smooth (left sagitta of paratype, holotype and referred specimen; Fig. 2e, f1, g1). A small posterodorsal projection is present. The predorsal portion can be rounded (Fig. 2e, g1) or displays a slight corner (Fig. 2f1, f2). The anterior margin is almost straight; the posterior margin is clearly incised beneath the posterodorsal projection. The preventral and posteroventral transitions are each regularly rounded. The ventral margin is almost straight or weakly curved and slightly to moderately crenulated. The sulcus is 'shoe-sole' shaped and comparatively short, as is characteristic for this genus (see generic diagnosis); the sulcus inclination angle is variable and ranges between 7.5° and 22°. A narrow crista inferior and a flat subcaudal iugum extend along the sulcus. The dorsal depression is relatively shallow, the ventral line clearly incised. For details of otolith measurements and otolith variables see Supplementary Data 3 and 4.

Two right lapilli could be photographed (Fig. 2f3, g2). They have an ovate shape with a straight lateral margin. The sulculus is well-defined and slightly steeper and longer on the lateral side than on the medial side.

Genus †***Alienagobius*** gen. nov.

Type and only species. †*Alienagobius pygmaeus* gen. et sp. nov.

Etymology. The name refers to the foreign ('aliena' in Latin) phenotypic appearance of the new taxon, and its general similarity to members of the Gobiidae. Gender masculine.

LSID ZooBank. This new genus is registered under https://zoobank.org/NomenclaturalActs/176CC3C6-25C1-4726-BB3E-1DD1F319E7F6.

Diagnosis. †*Alienagobius* gen. nov. is a small-sized, slender goby (SL up to 20.1 mm). Head moderately large (25–27% SL); caudal peduncle relatively long (24–26% SL); caudal fin approximately as long as head (23–26% SL) and slightly fan-shaped. Number of vertebrae 27 (10 + 17); length of abdominal part of vertebral column is 55–57% of that of caudal part. D1 with six spines, last spine distant from preceding one (distance is 4.5–5% SL); pterygiophore formula starts with 3–12 (further configuration not discernible). D2 with spine and 10–11 segmented rays; anal fin with spine and 11–12 segmented rays; caudal fin with 15–17 segmented rays (eight rays in the upper lobe). Number of pectoral-fin rays is 14; pelvic fins close together and probably not separated, each with spine and four rays. Pectoral girdle with four well developed radial bones of rounded-rectangular shape, with relatively big openings in-between. Relatively large and thick scales cover the middle and posterior parts of the body, while the abdominal body portion is almost scaleless. Scales seem to comprise both cycloid and ctenoid types; estimated number of scales in the longitudinal row is 44 (see Supplementary Data 3).

Sagitta rounded–squarish (LH 0.94–0.99) with a gently crenulated ventral margin; the posterodorsal projection is typically lacking (Fig. 2h–k). Sulcus short and 'shoe-sole' shaped, with flat subcaudal iugum. Its inclination ranges from 11° to 16°. The lapillus is egg-shaped (Fig. 2j2).

Remarks. Although a number of only four pelvic-fin rays is not the 'normal condition' in Gobioids, several species are known that have such a reduced number. Examples of the family Gobiidae are *Austrolethops* Whitley, 1935, some species of *Hetereleotris* Bleeker, 1874, e.g., *H. apora* (Hoese & Winterbottom, 1989) and *H. vinsoni* Hoese, 1986, all species of *Parioglossus* Regan, 1912 (Rennis & Hoese, 1985; Wang and Winterbottom 2006), and some species of *Eviota* Jenkins, 1903. Furthermore, the Microdesminae are characterized by a reduced number of only 2–4 pelvic-fin rays (Gill and Mooi 2010) and also *Milyeringa veritas* Whitley, 1945 (Milyeringidae) has only four pelvic-fin rays (Larson et al. 2013). Finally, the oldest fossil gobioid, †*Carlomonnius* Bannikov & Carnevale, 2016 has only four pelvic-fin rays (Bannikov and Carnevale 2016).

Differential diagnosis. The new genus †*Alienagobius* gen. nov. differs from both †*Moldavigobius* and †*Cryptograciles* gen. nov. in the presence of only four pelvic-fin rays (vs. five), a sagitta with a sulcus length (% OH), which is significantly lower than in †*Moldavigobius*, but significantly higher than in †*Cryptograciles* gen. nov. (One-way ANOVA, $p < 0.05$, Supplementary 4-part 1), and a lapillus with a more ovate shape and a more symmetrical contour of the sulculus (Fig. 2j2 vs. f3, g2; for the lapillus of †*Moldavigobius* see Reichenbacher and Bannikov 2023, fig. 1 d3). When compared solely to †*Moldavigobius*, additional characteristics of †*Alienagobius* gen. nov. include a D1-pterygiophore formula that starts with 3–12 (vs. 3–22), a higher number of flank scales in the longitudinal row (44 vs. < 30), a rounded-to-squarish sagitta (vs. rectangular) with a slightly crenulated ventral margin (vs. smooth), and significant differences in two otolith variables, i.e., a lower value in SuA and a higher

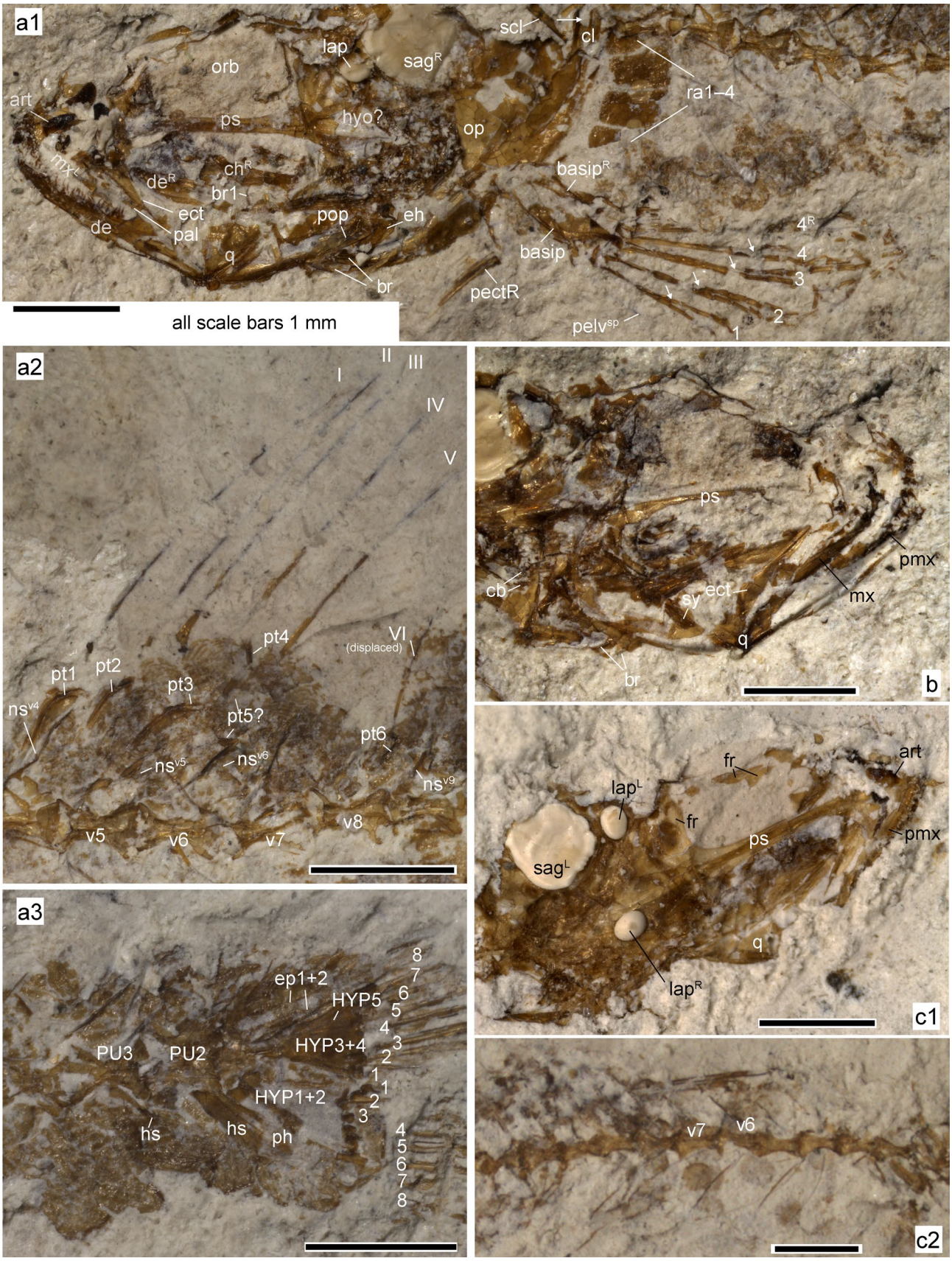
a1
orb
lap
sag^R
scl
cl
art
ps
hyo?
op
ra1–4
mx
de^R
ch^R
br1
basip^R
ect
de
pal
pop
eh
4^R
4
3
q
basip
br
pectR
2
pelv^sp
1
all scale bars 1 mm
a2
I
II
III
IV
V
pt4
VI
(displaced)
pt1
pt2
pt3
ns^v4
pt5?
pt6
ns^v5
ns^v6
ns^v9
v5
v6
v7
v8
b
ps
pmx
cb
sy
ect
mx
q
br
a3
ep1+2
HYP5
8
7
6
5
4
3
2
1
PU3
PU2
HYP3+4
HYP1+2
hs
hs
ph
c1
fr
art
lap^L
fr
ps
pmx
sag^L
q
lap^R
c2
v7
v6

◂**Fig. 8** Details of †*Alienagobius pygmaeus* gen. et sp. nov. from the Volhynian of Karpov Yar, near Naslavcea, northern Moldova. **a** Holotype counterpart (PIN 5274/68b); **a1** head and anteriormost body with pectoral and pelvic girdles (arrows at pelvic-fin rays indicate the points of their bifurcation); **a2** first dorsal fin spines I–VI, corresponding pterygiophores and pterygiophore insertion between neural spines; **a3** caudal skeleton and base of caudal-fin rays. **b** Head of holotype part (PIN 5274/68a). **c** Paratype (PIN 5274/43); **c1** head with left sagitta and both lapilli preserved in situ; **c2** anterior to middle part of body, note the almost lacking squamation. Superscripts L and R indicate bone from left and right body side respectively (when necessary). *art* articular process of premaxilla, *basip* basipterygium, *br* branchiostegal ray, *cb* ceratobranchial bones, *ch* anterior ceratohyal (displaced in a1), *cl* cleithrum (arrow indicates cleithral notch), *de* dentary, *ect* ectopterygoid, *eh* epihyal, *ep* epural, *fr* frontal bone, *hs* haemal spine, *hyo* hyomandibular, *HYP* hypural plate, *lap* lapillus, *mx* maxilla, *ns* neural spine, *op* opercle, *orb* orbit, *pal* palatine, *pectR* pectoral-fin rays, $pelv^{sp}$ pelvic fin spine, *ph* parhypural, *pmx* premaxilla, *pop* preopercle, *ps* parasphenoid, *pt* pterygiophore, *PU* preural vertebra, *q* quadrate, *ra* radials of pectoral girdle, *sag* sagitta, *scl* supracleithrum, *sy* symplectic, *v* vertebra. Numbers refer to ordinal numbers of branchiostegal rays, caudal-fin rays, D1 pterygiophores, epurals, pelvic-fin rays, radials and vertebrae, respectively

value in SuTipV (%OH). Likewise, when compared solely to †*Cryptograciles* gen. nov., further characteristic traits of †*Alienagobius* gen. nov. include a longer D2-base (24.9% SL vs. 19.6% SL), a slightly higher number of anal-fin rays (11–12 vs. 9–10), an almost scaleless abdominal part of the body (vs. dense squamation), pharyngeal teeth that are solely slender (vs. both thick and slender types), a premaxilla with a high articular process (vs. low), and significantly higher values in CoL (%OL) and SuL (%OL) (Figs. 2, 8; Table 2; Supplementary Data 3 and 4).

From the '*Lesueurigobius* look-alikes', with which †*Alienagobius* gen. nov. co-occurs at Karpov Yar (Reichenbacher and Bannikov 2022), the new taxon can be distinguished by its slightly fan-shaped caudal fin (vs. longish-lanceolate), fewer rays in the D2 (10–11 vs. 14–16), and the presence of rounded to squarish otoliths possessing a slightly crenulated ventral margin. From other previously described skeletal- and otolith-based marine and brackish fossil goby genera from the western Mediterranean and Paratethyan regions, †*Alienagobius* gen. nov. can be separated by its specific combination of body morphometric, meristic, and otolith characters (Gierl and Reichenbacher 2015; Schwarzhans et al. 2017, 2020a, b, 2022; Carolin et al. 2023; Dirnberger et al. 2024; Schwarzhans et al. 2024).

†*Alienagobius pygmaeus* gen. et sp. nov.
Figures 1d, 2h–j, k (cf.), 8
Type material. Holotype, PIN 5274/68a-b; 20.1 mm SL; somewhat incomplete part and well-preserved counterpart, with both sagittae and right lapillus preserved in situ. Two not very well preserved paratypes (PIN 1306/85b, PIN 5274/43, both in a single plate; Supplementary Data 6), each displaying the left sagitta and one (PIN 1306/85b) or both lapilli (PIN 5274/43) preserved in situ.

Referred material. Specimen PIN 5274/27b (shown in Supplementary Data 6) is referred to as †*A.* cf. *pygmaeus* gen. et sp. nov. Compared to the holotype and paratypes (see Supplementary Data 3), it possesses one ray less both in the D2 and the anal fin, one ray more in the caudal fin, a slightly more anteriorly inserted anal fin (opposite vertebra 11 vs. opposite vertebra 12/13), a slightly lower scale height (2.6–2.9% SL vs. 2.9–3.5% SL) and an otolith with a small posterodorsal projection (vs. no projection) (Fig. 2k).

Type locality and age. Karpov Yar ravine, Naslavcea, northern Moldova; upper Serravallian, lower Sarmatian sensu lato (Volhynian).

Etymology. The species epithet refers to the small size of this species, not exceeding about 20 mm.

LSID ZooBank. This new species is registered under https://zoobank.org/NomenclaturalActs/0E38BA61-DE10-4616-8D6F-BBEA1A2046B8.

Diagnosis. As described for the genus.

General description. A very small goby up to 20.1 mm SL with an elongated body outline (Fig. 1d, Supplementary Data 2 and 6). Number of vertebrae 27 (10 + 17); D1 with six spines, last spine distant from preceding one, D1-pterygiophore formula starting with 3–12; D2 with a spine and 11 segmented rays (10 in †*A.* cf. *pygmaeus*); anal fin with a spine and 12 segmented rays (11 in †*A.* cf. *pygmaeus*). Pectoral fin with about 14 rays. Pelvic fins close together, each with a spine and four rays that bifurcate after ca. 37% of their lengths. Caudal fin about as long as head, with 15–16 segmented rays (17 in †*A.* cf. *pygmaeus*); eight rays in the upper lobe. For further details see below and Supplementary Data 3.

Neurocranium. The neurocranium is preserved in lateral (holotype) or dorsolateral (paratypes) view (Fig. 8a1, b, c1). The frontal bones are long and narrow above the orbit and widened in a fan-shape posteriorly. The parasphenoid is straight, relatively narrow, and posteriorly broadened; details of the vomer are not visible. The ethmoid bones of the neurocranium are fragmented and no details are recognizable. Head scales seem to be absent.

Suspensorium, opercular apparatus, and hyoid arch. The suspensorium bones are mostly not well preserved. The symplectic is a robust rod in its lower portion (Fig. 8b), while the metapterygoid is not recognizable. The quadrate displays a triangular shape with a pronounced, wide indentation in its posterior part along with a well-developed posterior process (Fig. 8a1, b). The ectopterygoid exhibits an elongated, slightly triangular shape and extends towards the quadrate (Fig. 8b). There is no endopterygoid. The palatine shaft measures approximately half the length of the ectopterygoid (Fig. 8a1, also discernible in the paratype PIN 1306/85b). Although the palatine head potentially has a T-shaped configuration, definitive confirmation is hindered by preservation constraints. The opercle shape is triangular, tapering ventrally (Fig. 8a1), while other opercular bones remain obscured by overlapping bones, leaving only traces of the subopercle and the lower arm of the preopercle discernible.

The paratype PIN 1306/85b exhibits a right hyoid bar with four relatively well-preserved, robust branchiostegal rays, of which the last ray is separated by a small gap from the others. More anteriorly, the hyoid bar reveals two thin rays. However, these rays are not embedded on the same bedding plane and represent the first branchiostegal ray of the right and left hyoid bar, respectively. Consequently, there are a total of five branchiostegal rays. The epihyal is triangular; the interhyal is not recognizable.

Jaws. The mouth gape is moderately wide. The articulation of the lower jaw is positioned slightly anterior to the midpoint of the orbit (Fig. 8a1, b). The dentary is relatively slender and long (41% HL); the anguloarticular is relatively short and has a thin retroarticular process. The maxilla exhibits moderate width in its posterior half and is not spatulate. The premaxilla is moderately long and slender, nearly straight, featuring a prominent, elevated articular process; the ascending process is not well discernible (Fig. 8a1, c1). The postmaxillary process appears to be absent. Both the premaxilla and dentary display multiserial dentition, characterized by long, sharp, slender, curved teeth of varying sizes and thicknesses.

Branchial arches. Remains of the gill arches and gill rakers are preserved in the part of the holotype. The pharyngeal dentition comprises slender, conical teeth.

Vertebral column. The vertebral column consists of 27 vertebrae, with 10 abdominal vertebrae. The length of the abdominal part of the vertebral column comprises 55–57% of the length of the caudal part. Vertebral centra are elongated with distinctive constriction at the midpoint and typically slender neural spines (Fig. 8a2, c2). Parapophyses are discernible on the posterior abdominal vertebrae. Slender ribs extend from the third to the last abdominal vertebra; they are elongated from the third to the seventh vertebra, and then become gradually shorter. In the vicinity of the ribs, minute epineural bones are observable. The caudal vertebrae bear more or less equally inclined haemal spines.

Pectoral girdle and fins. The posttemporal comprises a flat main body and two processes, of which the anterior one is almost as long as the supracleithrum (well visible in PIN 1306/85b). The supracleithrum is elongate and robust. The cleithrum is strong, long and slightly curved; it has a 'cleithral notch' at its dorsal tip (indicated with arrow in Fig. 8a1). The radial bones of the pectoral girdle are well developed, of more or less rectangular shape and display round gapes in between (Figs. 1d, 8a1). The pectoral fin is preserved only in PIN 1306/85b and exhibits 14 rays.

Pelvic girdle and fins. The pelvic fins seem to be not separate and terminate far from the anal-fin origin (Fig. 1b). Their length is 16% SL. Each fin consists of a thin, moderately long spine and four rays; the rays bifurcate after ca. 37% of their lengths (Fig. 8a1, Supplementary Data 2). The basipterygii are slender and slightly curved.

Dorsal fins. The first dorsal fin comprises six slender spines. Spines I to IV are nearly of equal length (spine II is the longest), while spines V and VI, the latter being displaced in the holotype, gradually decrease in length (Fig. 8a2). While the D1-pterygiophore formula lacks clarity due to the state of preservation, the initial three pterygiophores suggest that it begins with 3–12 (Fig. 8a2).

The origin of the D2 occurs above vertebrae 11–12; it comprises a moderately long spine and 11 (10 in †*A.* cf. *pygmaeus* gen. et sp. nov.) segmented rays, of which the distal ends are not preserved. The first D2-pterygiophore inserts into the interneural space between the neural spines of the vertebrae nine and ten. The presence or absence of an interneural gap remains uncertain due to the distortion of the neural spines within this section of the abdominal part of the vertebral column.

Anal fin. The anal fin originates one vertebra behind the origin of D2, opposite to the vertebrae 12/13 (or vertebra 11 in †*A.* cf. *pygmaeus* gen. et sp. nov.). It comprises a moderately long spine (4.7% SL) and 12 rays (11 in †*A.* cf. *pygmaeus* gen. et sp. nov.). The number of anal-fin pterygiophores inserting before the first haemal spine is not discernible in the type specimens, whereas in †*A.* cf. *pygmaeus* gen. et sp. nov. this count is two.

Caudal endoskeleton and fin. The holotype and paratype PIN 1306/85b exhibit a relatively well-preserved caudal fin and

caudal endoskeleton. The caudal fin, constituting approximately 23–24% of SL, possesses a slightly fan-shaped structure comprised of 15–16 segmented and branched rays (17 in †*A.* cf. *pygmaeus* gen. et sp. nov.), with eight rays in the upper lobe. In the holotype, seven dorsal procurrent rays are discernible, whereas the ventral procurrent rays are not preserved. The caudal skeleton includes two relatively large hypural plates (HY1 + 2 and HY3 + 4) with the upper one fused to the terminal centrum; hypural 5 appears to be relatively elongated (Fig. 8a3). A distinctive gap separates the two hypural plates. The parhypural is more or less rectangular and as long as the hypaxial hypural plate. Although the preservation is rather poor, two relatively long and narrow epurals are identifiable as depicted in Fig. 8a3 and also observed in PIN 1306/85b.

The penultimate vertebra (PU2) presents a relatively short, triangular neural spine (best visible in PIN 1306/85b) and a broad, slightly curved, posteriorly expanded haemal spine (Fig. 8a3). PU3 and PU4 exhibit strongly inclined neural spines that are positioned closer together than those of the preceding vertebrae (Fig. 8a3, also apparent in PIN 1306/85b).

Scales. The abdominal section of the flank is almost scaleless and has only a few scattered cycloid scales (Figs. 1d, 8a1, c2; Supplementary Data 6). Small, rounded, cycloid scales cover the base of the D1, the belly, and the proximal part of the caudal-fin rays, where they are arranged in one or two vertical rows (Fig. 8a). The middle and posterior sections of the body (behind the vertebra 11) exhibit a squamation characterized by relatively large, thick flank scales with distinct radii and thickened posterior margins. In the paratype PIN 1306/85b, the flank scales are clearly ctenoid. In the holotype, the flank scale type is indistinct, but a few, minute, disseminated spinules possibly indicate detached ctenii.

Otoliths. The sagitta is rounded–squarish in shape (LH 0.94–0.99) with the highest point located in the middle or posterior region of the dorsal margin; the ventral margin is gently crenulated. The sagittae of the type specimens do not possess a posterodorsal projection (Fig. 2h, i, j1). The short sulcus is moderately inclined (11°–16°); the cauda is narrower than the ostium. The sulcus is accompanied by a straight or slightly curved crista inferior and flat subcaudal iugum. The egg-shaped lapillus exhibits a clearly defined sulculus with an almost symmetrical curvature along the medial and lateral margins (Fig. 2j2).

In contrast to the type specimens, the sagitta of specimen PIN 5274/27b shows a small posterodorsal projection (Fig. 2k), which is one of the reasons why this specimen is provisionally assigned to the species and designated †*A.* cf. *pygmaeus* gen. et sp. nov. (see "Referred material" above).

Phylogenetic results

We added †*Moldavigobius* spp. (combined data of †*M. helenae* and †*M. gloriae* sp. nov.), †*Cryptograciles* spp. (combined data of †*C. conicus* gen. et sp. nov. and †*C. robustus* gen. et sp. nov.), and †*Alienagobius pygmaeus* gen. et sp. nov. to the total evidence dataset of extant gobioid species from Dirnberger et al. (2024) to analyse the phylogenetic relationships of these new taxa using Bayesian inference. In the resulting tree, apart from the Gobiidae and Oxudercidae, all gobioid families are resolved as monophyletic, and their relationships are consistent with previous studies based on molecular data (see Supplementary Data 7). The Gobiidae and Oxudercidae are recovered as a clade with high support (PP 0.98), but several polytomies occurred within this clade, and the two families are not monophyletic. The three dwarf gobies were positioned in a polytomy with members of both the Gobiidae and Oxudercidae. A sister relationship was indicated between †*Alienagobius pygmaeus* gen. et sp. nov. and †*Moldavigobius* spp. (PP 0.58), though this relationship had low support.

Given these results, we followed the approach of Gierl et al. (2022), which recommends adding only one fossil taxon to the total evidence dataset when the inclusion of multiple fossils leads to the collapse of undoubtedly monophyletic clades (such as the Gobiidae and Oxudercidae). Accordingly, we conducted three separate Bayesian inference analyses, each including only one of the three dwarf goby taxa. In all cases, the gobioid families were recovered as monophyletic, and their relationships were consistent with previous molecular-based studies. The Gobiidae and Oxudercidae were well supported (PP 0.94–0.98), and the remaining families received maximal support values (PP 1) (Fig. 9a–c).

†*Moldavigobius* spp. was recovered within the Gobiidae, and positioned in a subclade (PP 0.85) that contains the European species *Gobius niger* Linnaeus, 1758, three Indo- or Indo-West-Pacific gobiids, and the European *Aphia* lineage. Within this subclade, †*Moldavigobius* spp. forms a weakly supported sister relationship with *Aphia minuta* (Risso, 1810) (PP 0.56), which is in turn sister to *Lesueurigobius sanzi* (de Buen, 1918). However, the support value for the *Aphia* lineage as a whole was low (PP 0.63).

Both †*Cryptograciles* spp. and †*Alienagobius pygmaeus* gen. et sp. nov. were resolved within the Oxudercidae, but in different subclades. †*Cryptograciles* spp. was recovered in a polytomy within a subclade (PP 0.73) that contains three lineages, i.e., the European *Pomatoschistus*, the northern Pacific *Acanthogobius* and the Indopacific *Mugilogobius* lineage (Fig. 9b). †*Alienagobius pygmaeus* gen. et sp. nov. was recovered within the *Stenogobius* lineage (PP 0.84), forming a sister relationship with the Western Atlantic species *Gobioides broussonnetii* Lacépède, 1800 (PP 0.78) (Fig. 9c).

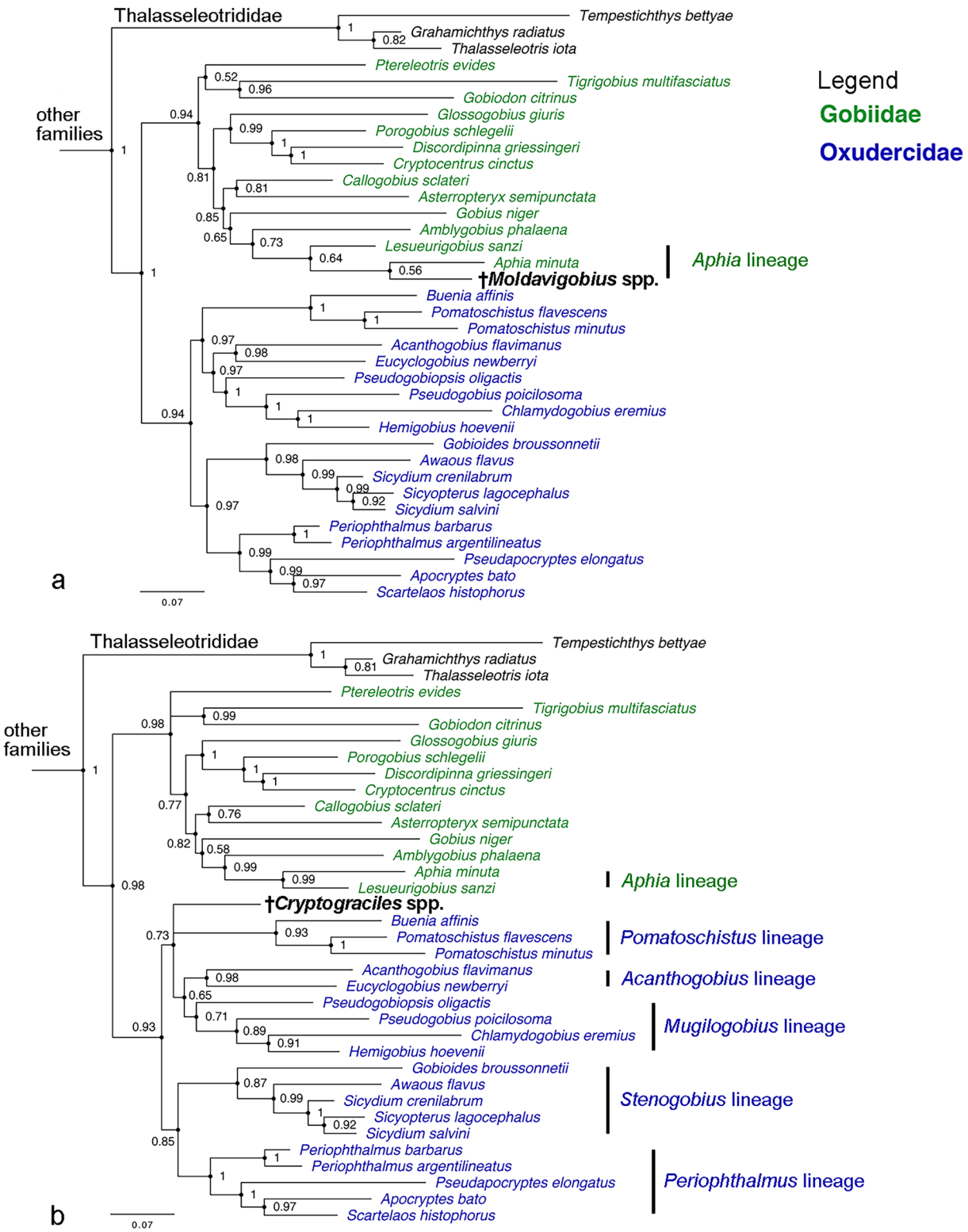

Fig. 9 Results of the total evidence Bayesian inference analyses (50% majority-rule consensus trees) based on 48 extant gobioid species (data from Dirnberger et al. 2024), with the addition of †*Moldavigobius* spp. (**a** ASDSF = 0.008738), †*Cryptograciles* spp. (**b** ASDSF = 0.007641) and †*Alienagobius pygmaeus* gen. et sp. nov. (**c** ASDSF = 0.017866). Values indicate posterior probabilities; scale bars depict average number of substitutions per site and character changes per character, respectively. *ASDSF* average standard deviation of split frequencies between two independent runs

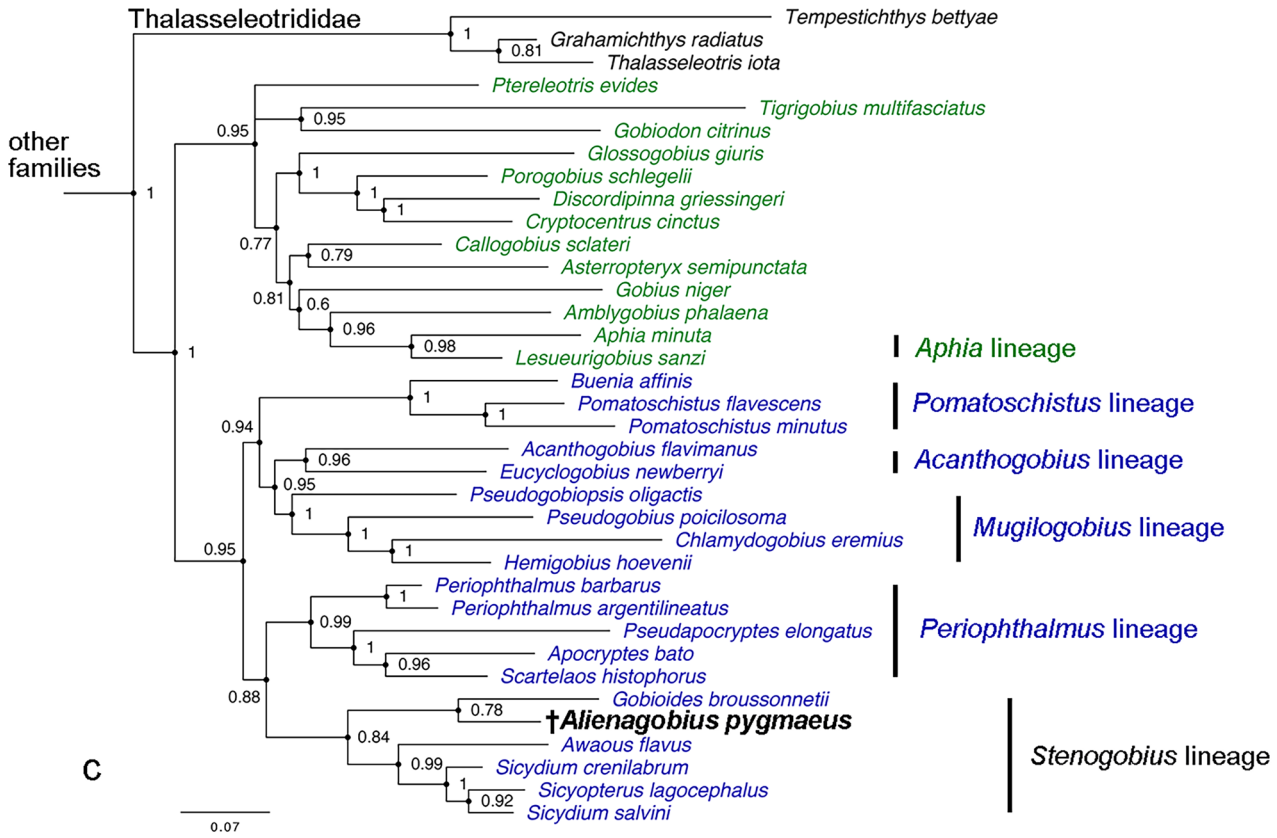

Fig. 9 (continued)

Discussion

Phylogenetic interpretation of the new dwarf gobies from Karpov Yar

The attribution of our three dwarf goby genera to the clade comprised by the families Gobiidae + Oxudercidae, as suggested by the Bayesian inference phylogenetic analyses (Fig. 9, Supplementary Data 7), can additionally be confirmed based on the comparative morphological approach. An important synapomorphy for the Gobiidae + Oxudercidae is the presence of five branchiostegal rays; all other extant gobioid families possess six branchiostegal rays (Wang et al. 2001; Gill and Mooi 2012). The presence of five branchiostegal rays could be confirmed for all three dwarf goby genera from Karpov Yar (for †*Moldavigobius* see Reichenbacher and Bannikov 2023, for the other two genera see section Systematic Palaeontology). Additional characters that are usually typical for the Gobiidae + Oxudercidae clade include a T-shaped palatine, absence of the endopterygoid, and presence of at least one interneural gap between the two dorsal fins (Akihito et al. 1984; Hoese 1984; Hoese and Gill 1993). These three traits can be confirmed for †*Moldavigobius* and †*Cryptogracilles* gen. nov., while the preservation of †*Alienagobius* gen. nov. only allowed to recognize the absence of the endopterygoid.

†*Moldavigobius*. Based on comparative morphology of its skeleton and otoliths, †*Moldavigobius* has previously been interpreted as a probable member of the European *Aphia* lineage within the family Gobiidae (Reichenbacher and Bannikov 2023). This is now additionally indicated by our phylogenetic analysis, in which †*Moldavigobius* is recovered within the *Aphia* lineage and in a sister-group relationship with *Aphia* Risso, 1827. Nevertheless, †*Moldavigobius* remains a *probable* fossil member of this lineage, since the posterior probability values for this relationship are low (Fig. 9a).

†*Cryptogracilles* gen. nov. The attribution of †*Cryptogracilles* gen. nov. to the family Oxudercidae, as suggested in the phylogenetic analysis, receives additional support from the comparative morphological approach. †*Cryptogracilles* gen. nov. has revealed a D1-pterygiophore formula that starts with 3–12, which is a derived character of the Oxudercidae, although exceptions exist (Harrison 1989; McKay and Miller 1997). In the Gobiidae as well as in other gobioid families the formula usually starts with 3–22 (Birdsong et al. 1988;

McKay and Miller 1997). Additionally, the presence of two epural bones in the caudal skeleton of †*Cryptogracciles* gen. nov. aligns with its attribution to the Oxudercidae; there are usually two epurals in Oxudercidae (plesiomorphic condition) and one in Gobiidae (derived) (Miller 1973; Birdsong et al. 1988; Harrison 1989).

In the phylogenetic tree shown in Fig. 9b, †*Cryptogracciles* gen. nov. is recovered in a polytomy with the *Pomatoschistus* lineage and a clade comprising members of the *Acanthogobius* and *Mugilogobius* lineage. In the following, we discuss whether the comparative morphological approach suggests a fit with any of these three lineages. Assignment of discussed extant species to the *Pomatoschistus* -, *Acanthogobius* – or *Mugilogobius* lineage is according to Agorreta et al. (2013).

Extant gobies of the *Pomatoschistus* lineage have at least 11 abdominal and 18 caudal vertebrae (vs. 10 + 17 in †*Cryptogracciles* gen. nov.), and many species have a reduced or absent postmaxillary process (Birdsong et al. 1988; McKay and Miller 1997), unlike the condition in †*Cryptogracciles* gen. nov., where this process is well developed (Fig. 7a2). On the other hand, the presence of two interneural gaps between the two dorsal fins, as seen in †*Cryptogracciles* gen. nov., often occurs in extant species of the *Pomatoschistus* lineage, while it is rare in other lineages (Birdsong et al. 1988; McKay and Miller 1997). Furthermore, there is some similarity between the otoliths of †*Cryptogracciles* gen. nov. and those of the 'sand gobies' among the *Pomatoschistus* lineage with respect to the small size of the cauda (see Gierl et al. 2018: fig. 3) and the low value (around 45%) of the otolith variable SuL (%OL) (see Supplementary Data 4; see Gierl et al. 2018: fig. 4 d). Nevertheless, there are also clear differences because none of the sand gobies of which the otoliths are known has rounded otoliths with finely to markedly crenulated margins, as is characteristic for †*Cryptogracciles* gen. nov. (see Gierl et al. 2018; Schwarzhans et al. 2020a).

Among the species of the *Acanthogobius* lineage, a highly elevated count in both abdominal and caudal vertebrae is usual, except in *Tridentiger* Gill, 1859a and *Rhinogobius* Gill, 1859b that mostly have a count of 10 + 16 (Birdsong et al. 1988). However, *Tridentiger* and *Rhinogobius* clearly differ from †*Cryptogracciles* gen. nov. (and most other Oxudercidae) by a D1-pterygiophore formula that starts with 3–22 (Birdsong et al. 1988). Additionally, †*Cryptogracciles* gen. nov. does not have tricuspid jaw teeth as is diagnostic for *Tridentiger* (see Cui et al. 2013), and its otoliths clearly differ from those of *Rhinogobius* in the more rounded shape, presence of crenulated margins, and smaller sulcus (see Gierl et al. 2018: fig. 2I–L).

The extant species of the *Mugilogobius* lineage have variable numbers of vertebrae, but the count 10 + 17 observed here is not common for them. This count has so far been reported solely for *Pseudogobius* Popta, 1922, and also in this genus it is an exception since the typical count is 10 + 16 (Birdsong et al. 1988). Moreover, a count of ten rays in the D2 and anal fin, as in †*Cryptogracciles* gen. nov., does not occur in *Pseudogobius*, which usually has seven (occasionally eight) rays in these fins (Larson and Hammer 2021).

In conclusion, †*Cryptogracciles* gen. nov. reveals a mosaic of characters, which is best fitting with its assignment to the sand gobies within the *Pomatoschistus* lineage but lacks the increased number of vertebrae of this group. Alternatively, †*Cryptogracciles* gen. nov. could represent a stem member of the *Pomatoschistus* lineage, which would also explain why the Bayesian analysis failed to unambiguously assign it to any of the extant clades.

†*Alienagobius* gen. nov. The assignment of †*Alienagobius* gen. nov. to the family Oxudercidae in our phylogenetic analysis receives support from the comparative morphological approach as has been discussed above for †*Cryptogracciles* gen. nov. Likewise, †*Alienagobius* gen. nov. shares with the Oxudercidae the derived condition of a D1-pterygiophore formula that starts with 3–12, and the presence of two epural bones in the caudal skeleton.

An interesting outcome of the phylogenetic analysis is the placement of †*Alienagobius* gen. nov. within the *Stenogobius* lineage (Fig. 9c). The extant species of this lineage share a global tropical distribution, but they do not occur in Europe, and fossils of this lineage are unknown. The vertebral count in the *Stenogobius* lineage is usually 10 + 16, with the 10 + 17 count, as seen in †*Alienagobius* gen. nov., being restricted to *Gobioides* Lacépède, 1800 (in which it is common), *Evorthodus* Gill, 1859c (rare), and *Ctenogobius* Gill, 1858 (rare) (Birdsong et al. 1988). In the following, we briefly discuss these three genera and whether †*Alienagobius* gen. nov. bears similarities with them.

Gobioides is represented now with five species which occur at the western Atlantic and eastern Pacific coasts of America (three species) and the eastern Atlantic coast of W-Africa (two species) (Murdy 1998; Froese and Pauly 2024). The species of *Gobioides* have an eel-like body, a continuous dorsal fin, a number of 14–21 rays in the dorsal and anal fins, a lanceolate caudal fin and a squamation consisting of numerous small cycloid scales (Murdy, 1998); *Gobioides* appears thus to be very different from †*Alienagobius* gen. nov.

The only members of *Evorthodus* are two species distributed allopatrically on both sides of the Isthmus of Panama (Rocha et al. 2005). They show some similarity with †*Alienagobius* gen. nov. in the body morphometry (but are not as elongate), in the presence of one ray more in the anal fin than in the D2, and in the counts of 11 and 12 rays, respectively, in these fins (Dawson 1967; Gilbert and Randall 1979; Smith 1997). On the other hand, their otoliths,

depicted in Schwarzhans and Aguilera (2024: fig. 42v–y), are clearly different from those of †*Alienagobius* gen. nov.

Pezold (2004) has re-validated *Ctenogobius*, previously considered as junior synonym of *Gobionellus*, and included 15 species in the genus. The biogeographic range of these species includes the western Atlantic and eastern Pacific coasts of America (14 species) and the eastern Central Atlantic region of W-Africa (one species), where they occur in freshwater, brackish, and also in marine environments (Froese and Pauly 2024). All 15 species have counts of lateral series scales ≤ 46 (Gilbert and Randall 1979; Pezold 2004) and the scales of the type species, *C. fasciatus* Gill, 1858, are reported as "finely ctenoid" (Regan 1906). Scale size and scale type of *Ctenogobius* are thus similar to those in †*Alienagobius* gen. nov. Further shared characters are presence of one more ray in the anal fin than in the D2 (Pezold 2004) and counts of 10–12 rays in the D2 and 11–13 rays in the anal fin (data compiled from Froese and Pauly 2024). Nevertheless, the otoliths of *Ctenogobius*, shown in Schwarzhans and Aguilera (2024: fig. 42), are either long-rectangular or high-rectangular, and their sulcus is larger and more inclined as in †*Alienagobius* gen. nov.

In conclusion, we cannot discern a relationship of †*Alienagobius* gen. nov. with any extant genera of the *Stenogobius* lineage based on comparative morphology. The biogeographic distribution of these genera and the present-day members of the *Stenogobius* lineage also do not hint to such a relationship; however, the result of the phylogenetic analysis may indicate that the biogeographic history of this lineage could be more complex as the present-day distribution indicates (see Thacker 2015; Reichenbacher and Přikryl 2024).

Remarks on the palaeoenvironment

In the Karpov Yar ravine in the north of Moldova, the upper Serravallian (lower Sarmatian sensu lato, Volhynian) strata unconformably overlie Cretaceous conglomerates and cherts (Ionko 1954; Yakubovskaya 1955), and the clay at their base is overflowing with leaves of terrestrial plants. Apparently, these are deposits of coastal swamps, as evidenced by the discovery of a spade-footed toad there in 2007. The overlying diatomites and marls clearly belong to lagoonal deposits, as indicated by several thin layers with evidence of mass mortality of fishes; all fish discoveries are limited to these layers. There are no mass-mortality layers further up in the outcrop, and presence of marine molluscs indicates a marine transgression in this place by the late Serravallian (early Sarmatian sensu lato, Volhynian) (Bannikov 2019; Reichenbacher and Bannikov 2022).

In terms of the number of finds, gobies of the Karpov Yar locality concede only to the pelagic silversides (†*Atherina suchovi* Switchenska, 1973) and herrings (†*Moldavichthys switshenskae* Baykina & Schwarzhans, 2017). At the same time, their systematic diversity is exceptionally high. Other bottom-dwelling fishes of the Karpov Yar locality, on the contrary, are quite rare: they are known to date only from a few finds of clinid blennies, even less abundant flounders and pipefishes, and a single specimen of scorpionfish.

Why do the dwarf gobies from Karpov Yar exhibit minimal skeletal differences?

As discussed above, the three dwarf goby genera from the early Sarmatian of Karpov Yar belong to different families and lineages, with †*Moldavigobius* being part of the Gobiidae and †*Cryptograciles* and †*Alienagobius* placed within different clades of the Oxudercidae (Fig. 9). It is surprising that these three genera show low morphological disparity, particularly in vertebrae numbers (all have 10 + 17 vertebrae), and limited variation in body morphometry and fin-ray counts (Fig. 10a, Table 2, Supplementary Data 3). Given their distant phylogenetic relationships, it is unlikely that these similarities in skeletal features are due to genetic constraints. Instead, it is more plausible that they result from adaptations to similar microhabitats (see Moen et al. 2013; Cerca et al. 2019). Their small size and nearly identical skeletal and body morphologies may have been optimized for the specific environmental conditions at Karpov Yar, such as interacting with a slightly muddy substrate and low hydrodynamic turbidity (as inferred from the prevalence of diatomites and marls).

Moreover, the presence of five dwarf goby species (two species of †*Moldavigobius*, two of †*Cryptograciles* gen. nov., one of †*Alienagobius* gen. nov.), together with six species of relatively larger gobies resembling *Lesueurigobius* (see Reichenbacher and Bannikov 2022), suggests that the Karpov Yar locality was ecologically more heterogeneous than the lithofacies might indicate. As seen in extant dwarf gobies (Tornabene et al. 2013; Brandl et al. 2018), a cryptobenthic lifestyle is likely for the fossil dwarf gobies, with each genus and species adapted to specific micro-niches within available microhabitats. This could also explain their relatively high species diversity, as small body size in cryptobenthic fish has been linked to increased diversification rates (Brandl et al. 2018).

Among the three dwarf goby genera, notable differences are evident in scale size, longitudinal scale row counts, scale ornamentation (number of radii), and otolith (sagitta and lapillus) morphology (Fig. 10a, for details see Differential diagnoses for genera). Scales play key roles in structural robustness, swimming efficiency, and predator avoidance via mechanical protection or reflection (Helfman et al. 2009; Zhu et al. 2012; Vernerey and Barthelat 2014), while otoliths are part of the inner ear and are crucial for balance, sound

Morphological differences between the dwarf goby genera from Karpov Yar		†*Moldavigobius* vs. †*Cryptograciles* gen. nov.	†*Moldavigobius* vs. †*Alienagobius* gen. nov.	†*Cryptograciles* gen. nov. vs. †*Alienagobius* gen. nov.
Jaws, teeth	Pharyngeal dentition			▲
	Pmx articular proc.			▲
Morphometry	D2-base (% SL)			▲
Meristics	D1-pteryg. formula	▲	▲	
	Anal-fin rays	▲		▲
	Pelvic-fin rays		▲	▲
Squamation	Scale height (% SL)	▲		
	Longit. scale number	▲	▲	
	Density scale cover			▲
Sagitta variables	CoL (%OL)	▲		▲
	SuAngle		▲	
	SuL (%OL)	▲		▲
	SuL (%OH)	▲	▲	▲
	SuH (%OL)	▲		
	SuH (%OH)	▲		
	SuTipV (%SuEndV)	▲		
	SuTipV (%OH)	▲	▲	
Lapillus	Overall shape	▲	▲	▲
	Sulculus	▲	▲	▲

a

Morphological differences between congeneric dwarf goby species from Karpov Yar		†*M. gloriae* vs. †*M. helenae*	†*M. gloriae* vs. †*M. suavis*	†*M. helenae* vs. †*M. suavis*	†*C. conicus* vs. †*C. robustus*
Neurocranium	Shape frontals	Unknown	No data (*M. suavis* is otolith-based)	No data (*M. suavis* is otolith-based)	▲
Suspensorium	Shape opercle	Unknown			▲
Morphometry	Length lower jaw	▲			
	BD2	▲			
	abdVc (%caudVc)				▲
Meristics	D2-rays				▲
	Pectoral-fin rays	Unknown in *M. gloriae*			▲
	Insertion anal fin	▲			
Squamation	Radii flank scale	▲			
Sagitta variables	CoL (%OL)			▲	
	SuL (%OL)				▲
	SuL (%OH)		▲		▲

b

Fig. 10 Morphological differences between dwarf goby genera (**a**) and their species (**b**) from Karpov Yar, near Naslavcea, northern Moldova. Morphometric variables are considered significantly different if they differ by ≥ 5% SL. Differences in otolith variables were analysed using one-way ANOVA with posthoc tests ($p < 0.05$) for the three genera and the three †*Moldavigobius* species, and using *T*-test (with Monte Carlo permutation, $p < 0.05$) for the two †*Cryptograciles* species. Grey shading indicates variables that distinguish two or all three groups from each other. For details of data see Supplementary Data 3 and 4

localization, and acoustic communication (Popper et al. 2005; Horvatić et al. 2021). Based on the references mentioned, we assume that differences in scales and otoliths may be related to improved performance within specific microniches. This could explain why scale and otolith morphometry vary significantly between our genera (see section Results and Fig. 10, see statistical results in Supplementary Data 4), while the constraints of the shared habitat led to minimal disparity in skeletal traits. Such a pattern of divergent otolith morphology coupled with absence of other morphological traits is well known for another group of small-sized fishes, which is the Aphaniidae (tooth carps) (e.g.Teimori et al. 2012; Charmpila et al. 2024), but the underlying processes are still matter of future research.

Another interesting observation is that sagitta differences between congeneric species are less pronounced than those between genera, but that other taxonomic traits distinguish the species (Fig. 9b). Some, like differing lower jaw lengths between †*M. gloriae* sp. nov. and †*M. helenae*, or opercle shape differences between †*C. conicus* gen. et sp. nov. and †*C. robustus* gen. et sp. nov., are likely linked to feeding strategies. Others, such as variations in anal-fin insertion between †*M. gloriae* sp. nov. and †*M. helenae*, or differences in D2 and pectoral fin-ray counts between †*C. conicus* gen.

et sp. nov. and †*C. robustus* gen. et sp. nov., may reflect adaptations for maneuverability.

In conclusion, dwarf goby diversification at Karpov Yar appears to have been driven by adaptation to different microniches with improved swimming efficiency (derived from scale and fin variation), auditory perception (derived from otolith variation), and adaptation to particular dietary niches. Evidence for the latter process is not only indicated by differences in jaw length and opercle shape between congeneric species (see above), but also by differences in the jaw and suspensory bones between genera, i.e., premaxilla with high articular process in †*Alienagobius* gen. nov. (Fig. 8a1) vs. low articular process in †*Cryptograciles* gen. nov. (Fig. 7a2), and solely slender pharyngeal teeth in †*Alienagobius* gen. nov. vs. both thick and slender types in †*Cryptograciles* gen. nov.

Only because the new fossil taxa were at least partially exceptionally well-preserved and the otoliths were preserved in situ it was possible to recognize their taxonomic and phylogenetic diversity. In other words: all four new species described here would otherwise probably have been grouped together under one and the same species name.

Conclusion

The discovery of a taxonomically diverse assemblage of dwarf gobies from Karpov Yar indicates high ecological complexity of the late Serravallian (early Sarmatian sensu lato, Volhynian) coastal ecosystems in this part of the Eastern Paratethys. Despite their distinct phylogenetic positions—spanning both the families Gobiidae and Oxudercidae—the morphological similarities observed among these dwarf gobies suggest convergent evolution driven by habitat-specific selective pressures. The shared skeletal traits and body morphometry across the genera likely reflect adaptations to similar cryptobenthic lifestyles in a low-energy, muddy, lagoonal environment. Nevertheless, clear differences in fin positions, fin-ray counts, bones of the jaw and suspensorium as well as scale and sagitta and lapillus morphology between genera and species indicate adaptations to particular microniches and highlights the significance of scale and otolith morphology in elucidating taxonomic diversity in fossils.

The findings suggest that Karpov Yar was an ecologically dynamic site that provided diverse microhabitats that enabled the coexistence of multiple cryptobenthic goby species. These results not only advance our understanding of goby evolution and paleoecology but also underscore the importance of exceptional fossil preservation, which in this case allowed for a detailed taxonomic and phylogenetic reconstruction that would otherwise have been impossible.

Supplementary Information The online version contains supplementary material available at https://doi.org/10.1007/s12542-025-00726-z.

Acknowledgements We thank Dr. Doug Hoese (Sydney, Australia), Dr. Helen Larson (Darwin, Australia) and Dr. Roland Fricke (Stuttgart, Germany) for helpful comments and sharing literature that was difficult to find, and Dr. W. Schwarzhans (Hamburg, Germany) for constructive discussion on otolith variability and for sharing photos of unpublished otolith material from his collection. We thank Ulrich Schliewen (Munich, Germany) for constructive discussion on character distribution in Gobiidae and Oxudercidae and the reviewers for constructive remarks. Finally, we are indebted for the photographs to Mrs. S.V. Bagirov (PIN) (Figs. 1, 4a1, Supplementary Data 2) and R.A. Rakitov (PIN) (Fig. 2i). The authors have no conflict of interest to declare.

Funding Open Access funding enabled and organized by Projekt DEAL. Partial financial support was received from the Department of Earth and Environmental Sciences, LMU Munich.

Data availability statement All relevant data are within the manuscript and the Supplementary Data 1–7. The data files (nexus format) of the phylogenetic analyses can be found online at figshare: https://figshare.com/account/home#/projects/244994.

Declarations

Conflict of Interests The authors have no competing interests to declare that are relevant to the content of this article.

References

Agorreta, A., San Mauro, D., Schliewen, U., Van Tassell, J. L., Kovačić, M., Zardoya, R., & Rüber, L. (2013). Molecular phylogenetics of Gobioidei and phylogenetic placement of European gobies. *Molecular Phylogenetics and Evolution, 69*(3), 619–633. https://doi.org/10.1016/j.ympev.2013.07.017

Akihito, Hayashi, M., Yoshino, T., ShimadaYamamoto, K. T., & Senou, H. (1984). Suborder Gobioidei. In H. Masuda, K. Amaoka, C. Araga, T. Uyeno, & T. Yoshino (Eds.), *The fishes of the Japanese archipelago* (pp. 236–289). Tokyo: Tokai University Press.

Bannikov, A. F. (2019). Early Sarmatian (Volhynian) bony fishes of the Eastern Paratethys [Rannesarmatskiye (volynskiye) kostistye ryby Vostochnogo Paratetisa]. *Morphological evolution and stratigraphic problems. Materials of LXIV session of the Paleontological society* (pp. 207–209). St Petersburg: VSEGEI.

Bannikov, A.F. & Carnevale, G. 2016. †*Carlomonnius quasigobius* gen. et sp. nov.: the first gobioid fish from the Eocene of Monte Bolca, Italy. *Bulletin of Geosciences, 91*(1), 13–22.

Baykina, E. M., & Schwarzhans, W. W. (2017). Review of "*Clupea humilis*" from the Sarmatian of Moldova and description of *Moldavichthys switshenskae* gen. et sp. nov. *Swiss Journal of Palaeontology, 136*(1), 141–149. https://doi.org/10.1007/s13358-016-0121-6

Birdsong, R. S., Murdy, E. O., & Pezold, F. L. (1988). A study of the vertebral column and median fin osteology in gobioid fishes with comments on gobioid relationships. *Bulletin of Marine Science, 42*(2), 174–214.

Bleeker, P. (1849). Bijdrage tot de kennis der ichthyologische fauna van het eiland Madura: met beschrijving van eenige nieuwe soorten. *Verhandelingen van het Bataviaasch Genootschap der Kunsten en Wetenschappen.* (Vol. 22). Batavia: Lange & Co.

Bleeker, P. (1856). Beschrijvingen van nieuwe of weinig bekende vischsoorten van Manado en Makassar, grootendeels verzameld op eene reis naar den Molukschen Archipel in het gevolg van den Gouverneur Generaal Duymaer van Twist. *Acta Societatis Regiae Scientiarum Indo-Neêrlandicae, 1*(6), 1–80.

Bleeker, P. (1859). Enumeratio specierum piscium hucusque in Archipelago Indico. *Acta Societatis Scientiarum Indo-Neerlandensis, 6*, 1–276.

Bleeker, P. (1874). Equisse d'un système naturel des Gobioides. *Archives Néerlandaises des sciences exactes et naturelles, 9*(4), 289–331.

Brandl, S. J., Goatley, C. H. R., Bellwood, D. R., & Tornabene, L. (2018). The hidden half: Ecology and evolution of cryptobenthic fishes on coral reefs. *Biological Reviews, 93*(4), 1846–1873. https://doi.org/10.1111/brv.12423

Carolin, N., Bajpai, S., Maurya, A. S., & Schwarzhans, W. (2023). New perspectives on late Tethyan Neogene biodiversity development of fishes based on Miocene (~ 17 Ma) otoliths from southwestern India. *PalZ, 97*(1), 43–80. https://doi.org/10.1007/s12542-022-00623-9

Cerca, J., Meyer, C., Stateczny, D., Siemon, D., Wegbrod, J., Purschke, G., Dimitrov, D., & Struck, T. H. (2019). Deceleration of morphological evolution in a cryptic species complex and its link to paleontological stasis. *Evolution, 74*(1), 116–131. https://doi.org/10.1111/evo.13884

Charmpila, E. A., Teimori, A., & Reichenbacher, B. (2024). Otolith-based species identification in the killifish *Aphaniops* (Teleostei; Cyprinodontiformes; Aphaniidae) using both morphometry and wavelet analysis. *Acta Zoologica Online First*. https://doi.org/10.1111/azo.12518

Cui, R., Pan, Y., Yang, X., & Wang, Y. (2013). A new barbeled goby from south China (Teleostei: Gobiidae). *Zootaxa, 3670*(2), 177–192. https://doi.org/10.11646/zootaxa.3670.2.4

Cuvier, G. (1816). *Le Règne Animal distribué d'après son organisation pour servir de base à l'histoire naturelle des animaux et d'introduction à l'anatomie comparée. Tome II, Les reptiles, les poissons, les mollusques et les annélides*. Paris: A. Belin.

Cuvier, G., & Valenciennes, A. (1837). *Histoire Naturelle des Poissons—Tome douzième. Suite du livre quatorzième. Gobioïdes. Livre quinzième. Acanthoptérygiens à pectorales pédiculées*. Paris: Levrault, F. G.

Dawson, C. E. (1967). Notes on species of the goby genus *Evorthodus*. *Copeia, 1967*(4), 855–857.

de Buen, F. (1918). Los Góbidos de la Península Ibérica y Baleares. Nota II. Catálogo sistemático y ensayo de distríbución geográfica. *Boletin de pescas, 26*, 291–337.

de Buen, F. (1928). Descripción de un nuevo *Gobius* (*G. roulei* nov. sp.). *Notas y résumenes, Instituto Español de Oceanografia; Ministerio de Marin Madrid (Ser. 2), 30*, 1–6.

Dirnberger, M., Bauer, E., & Reichenbacher, B. (2024). A new freshwater gobioid from the Lower Miocene of Turkey in a significantly amended total evidence phylogenetic framework. *Journal of Systematic Palaeontology, 22*(1), 2340498. https://doi.org/10.1080/14772019.2024.2340498

Froese, R., Pauly, D. (2024). FishBase. World Wide Web electronic publication. www.fishbase.org, version (06/2024). www.fishbase.org.

Gierl, C., Dohrmann, M., Keith, P., Humphreys, M., Esmaeili, H. R., Vukić, J., Šanda, R., & Reichenbacher, B. (2022). An integrative phylogenetic approach for inferring relationships of fossil gobioids (Teleostei: Gobiiformes). *PLoS ONE, 17*(7), e0271121. https://doi.org/10.1371/journal.pone.0271121

Gierl, C., Liebl, D., Šanda, R., Vukić, J., Esmaeili, H. R., & Reichenbacher, B. (2018). What can goby otolith morphology tell us? *Cybium, 42*(4), 349–363. https://doi.org/10.26028/cybium/2018-424-006

Gierl, C., & Reichenbacher, B. (2015). A new fossil genus of Gobiiformes from the Miocene characterized by a mosaic set of characters. *Copeia, 103*(4), 792–805. https://doi.org/10.1643/ci-14-146

Gilbert, C. R., & Randall, J. E. (1979). Two new western Atlantic species of the gobiid fish genus *Gobionellus*, with remarks on characteristics of the genus. *Gulf of Mexico Science, 3*(1), 27–47.

Gill, A. C., & Mooi, R. D. (2010). Character evidence for the monophyly of the Microdesmidae, with comments on relationships to *Schindleria* (Teleostei: Gobioidei: Gobiidae). *Zootaxa, 2442*, 51–59.

Gill, A. C., & Mooi, R. D. (2012). Thalasseleotrididae, new family of marine gobioid fishes from New Zealand and temperate Australia, with a revised definition of its sister taxon, the Gobiidae (Teleostei: Acanthomorpha). *Zootaxa, 3266*(1), 41–52. https://doi.org/10.11646/zootaxa.3266.1.3

Gill, T. (1858). Synopsis of the fresh water fishes of the western portion of the island of Trinidad, W. I. *Annals of the Lyceum of Natural History of New York, 6*, 363–430.

Gill, T. (1859a). IV.—Prodromus descriptionis familiae Gobioidarum duorum generum novorum. *Annals of the Lyceum of Natural History of New York, 7*(1–3), 16–21.

Gill, T. (1859b). Notes on a collection of Japanese fishes, made by Dr. J. Morrow. *Proceedings of the Academy of Natural Sciences of Philadelphia, 11*, 144–150.

Gill, T. (1859c). Description of a type of gobioids intermediate between Solinae and Tridentigerinae. *Proceedings of the Academy of Natural Sciences of Philadelphia, 11*, 195–196.

Günther, A. (1861). *Catalogue of the fishes in the British museum. Catalogue of the acanthopterygian fishes in the collection of the British museum* (Vol. 3). London: British Museum of Natural History.

Gut, C., Vukić, J., Šanda, R., Moritz, T., & Reichenbacher, B. (2020). Identification of past and present gobies: Distinguishing *Gobius* and *Pomatoschistus* (Teleostei: Gobioidei) species using characters of otoliths, meristics and body morphometry. *Contributions to Zoology, 89*, 282–323. https://doi.org/10.1163/18759866-bja10002

Hammer, Ø., Harper, D. A. T., & Ryan, P. D. (2001). PAST: Paleontological statistics software package for education and data analysis. *Palaeontologia Electronica, 4*(1), 1–9.

Harrison, I. J. (1989). Specialization of the gobioid palatopterygoquadrate complex and its relevance to gobioid systematics. *Journal of Natural History, 23*(2), 325–353. https://doi.org/10.1080/00222938900770211

Heckel, J. J. (1837). Ichthyologische Beiträge zu den Familien der Cottoiden, Scorpaenoiden, Gobioiden und Cyprinoiden. *Annalen des Wiener Museums der Naturgeschichte, 2*(1), 143–164.

Helfman, G. S., Collette, B. B., Facey, D. E., & Bowen, B. W. (2009). *The diversity of fishes: Biology, evolution, and ecology* (2nd ed.). Wiley-Blackwell.

Hoese, D. F. (1984). Gobioidei: relationships. In H. G. Moser, W. J. Richards, D. M. Cohen, M. P. Fahay, A. W. Kendall Jr., & S. L. Richardson (Eds.), *Ontogeny and systematics of fishes* (pp. 588–591). Gainesville: American Society of Ichthyologists and Herpetologists.

Hoese, D. F. (1986). Descriptions of two new species of *Hetereleotris* (Pisces: Gobiidae) from the western Indian ocean, with discussion of related species. *The J.L.B Smith Institute of Ichthyology Special Publication, 41*, 1–25.

Hoese, D. F., & Gill, A. C. (1993). Phylogenetic relationships of eleotridid fishes (Perciformes, Gobioidei). *Bulletin of Marine Science, 52*(1), 415–440.

Hoese, D. F., & Winterbottom, R. (1979). A new species of *Lioteres* (Pisces, Gobiidae) from Kwazulu, with a revised checklist of South African gobies and comments on the generic relationships and endemism of western Indian ocean gobioids. *Royal Ontario Museum Life Sciences Occasional Paper, 31*, 1–13.

Horvatić, S., Malavasi, S., Vukić, J., Šanda, R., Marčić, Z., Ćaleta, M., Lorenzoni, M., Mustafić, P., Buj, I., & Onorato, L. (2021). Correlation between acoustic divergence and phylogenetic distance in soniferous European gobiids (Gobiidae; Gobius lineage). *PLoS ONE, 16*(12), e0260810.

Ionko, V. I. (1954). O nakhodke iskopayemykh ryb v nizhnesarmatskikh otlozheniyakh MSSR. *Trudy Odesskogo Universiteta. Sbornik Geologo-Geograficheskogo Fakul'teta, 2*, 109–119.

Jenkins, O. P. (1903). Report on collections of fishes made in the Hawaiian islands, with descriptions of new species. *Bulletin of the U.S. Fish Commission, 22*(1902), 417–511.

Kovačić, M., & Šanda, R. (2016). A new species of *Gobius* (Perciformes: Gobiidae) from the Mediterranean Sea and the redescription of *Gobius bucchichi*. *Journal of Fish Biology, 88*(3), 1104–1124. https://doi.org/10.1111/jfb.12883

Lacépède, B. G. E. (1800). *Histoire naturelle des poissons*. Plassan.

Larson, H. K., Foster, R., Humphreys, W. F., & Stevens, M. I. (2013). A new species of the blind cave gudgeon *Milyeringa* (Pisces: Gobioidei, Eleotridae) from Barrow Island, Western Australia, with a redescription of *M. veritas* from Whitley. *Zootaxa, 3616*(2), 135–150. https://doi.org/10.11646/zootaxa.3616.2.3

Larson, H. K., & Hammer, M. P. (2021). A revision of the gobiid fish genus *Pseudogobius* (Teleostei, Gobiidae, Tridentigerinae), with description of seven new species from Australia and South-east Asia. *Zootaxa, 4961*(1), 1–85. https://doi.org/10.11646/zootaxa.4961.1.1

Linnaeus, C. (1758). *Systema Naturae, 10th edition (Systema naturae per regna tria naturae, secundum classes, ordines, genera species, cum characteribus, differentiis, synonymis, locis. Tomus I. Editio decima, reformata)* (10 Aufl). Holmia: Laurentius Salvius.

McKay, S. I., & Miller, P. J. (1997). The affinities of European sand gobies (Teleostei: Gobiidae). *Journal of Natural History, 31*(10), 1457–1482. https://doi.org/10.1080/00222939700770791

Miller, M. A., Pfeiffer, W., & Schwartz, T. (2010). Creating the CIPRES science gateway for inference of large phylogenetic trees. *2010 gateway computing environments workshop (GCE).* New Orleans: IEEE.

Miller, P. J. (1973). The osteology and adaptive features of *Rhyacichthys aspro* (Teleostei: Gobioidei) and the classification of gobioid fishes. *Journal of Zoology, 171*(3), 397–434. https://doi.org/10.1111/j.1469-7998.1973.tb05347.x

Miller, P. J. (2004). *The freshwater fishes of Europe* (Vol. 8/II). Wiebelsheim: AULA-Verlag.

Miller, P. J., & El-Tawil, M. Y. (1974). A multidisciplinary approach to a new species of *Gobius* (Teleostei: Gobiidea) from southern Cornwall. *Journal of Zoology, 174*(4), 539–574. https://doi.org/10.1111/j.1469-7998.1974.tb03181.x

Miller, P. J., & Šanda, R. (2008). A new West Balkanian sand-goby (Teleostei: Gobiidae). *Journal of Fish Biology, 72*(1), 259–270. https://doi.org/10.1111/j.1095-8649.2007.01709.x

Moen, D. S., Irschick, D. J., & Wiens, J. J. (2013). Evolutionary conservatism and convergence both lead to striking similarity in ecology, morphology and performance across continents in frogs. *Proceedings of the Royal Society B-Biological Sciences*. https://doi.org/10.1098/rspb.2013.2156

Murdy, E. O. (1998). A review of the gobioid fish genus *Gobioides*. *Ichthyological Research, 45*(2), 121–133. https://doi.org/10.1007/bf02678554

Near, T. J., & Thacker, C. E. (2024). Phylogenetic classification of living and fossil ray-finned fishes (Actinopterygii). *Bulletin of the Peabody Museum of Natural History, 65*(1), 3–302.

Nelson, J. S., Grande, T. C., & Wilson, M. V. H. (2016). *Fishes of the world* (5th ed.). John Wiley & Sons inc.

Pallas, P. S. (1814). *Zoographia Rosso-Asiatica, sistens omnium animalium in extenso Imperio Rossico et adjacentibus maribus observatorum recensionem, domicilia, mores et descriptiones anatomen atque icones plurimorum* (Vol. 3). Sankt Petersburg: Academia Scientiarum.

Pezold, F. (2004). Phylogenetic analysis of the genus *Gobionellus* (Teleostei: Gobiidae). *Copeia, 2004*(2), 260–280. https://doi.org/10.1643/CI-02-218R3

Popper, A. N., Ramcharitar, J., & Campana, S. E. (2005). Why otoliths? Insights from inner ear physiology and fisheries biology. *Marine & Freshwater Research, 56*(5), 497–504. https://doi.org/10.1071/MF04267

Popta, C. M. L. (1922). Vierte und letzte Fortsetzung der Beschreibung von neuen Fischarten der Sunda-Expeditio. *Zoologische Mededeelingen (Leiden), 7*, 27–39.

Rambaut, A. (2018). FigTree. Tree figure drawing tool version 1.4.4. http://tree.bio.ed.ac.uk/software/figtree/. Edinburgh: University of Edinburgh.

Regan, C. T. (1906). On the fresh-water fishes of the island of Trinidad, based on the collection, notes, and sketches made by Mr. Lechmere Guppy, Junr. *Proceedings of the Zoological Society of London, 1906*, 378–393.

Regan, C. T. (1912). New fishes from Aldabra and Assumption, collected by Mr. J. C. F. Fryer. *Transactions of the Linnean Society of London, Series 2, Zoology, 15*(2), 301–302.

Reichenbacher, B., & Bannikov, A. F. (2022). Diversity of gobioid fishes in the late middle Miocene of northern Moldova, Eastern Paratethys—part I: An extinct clade of *Lesueurigobius* look-alikes. *PalZ, 96*, 67–112. https://doi.org/10.1007/s12542-021-00573-8

Reichenbacher, B., & Bannikov, A. F. (2023). Diversity of gobioid fishes in the late middle Miocene of northern Moldova, Eastern Paratethys—part II: Description of †*Moldavigobius helenae* gen. et sp. nov. *PalZ, 97*, 365–381. https://doi.org/10.1007/s12542-022-00639-1

Reichenbacher, B., & Přikryl, T. (2024). Revision and phylogenetic placement of one of the earliest freshwater gobies from the Lower Oligocene of Central Europe. *Historical Biology*. https://doi.org/10.1080/08912963.2024.2406964

Reichenbacher, B., Vukić, J., Šanda, R., Schliewen, U. K., Esmaeili, H. R., & Kassar, A. (2023). Skeletal traits and otoliths can unravel the relationships within European Gobiidae (*Gobius* lineage sensu lato). *Zoological Journal of the Linnean Society, 199*, 656–687. https://doi.org/10.1093/zoolinnean/zlad058

Rennis, D. S., & Hoese, D. F. (1985). A review of the genus *Parioglossus*, with description of six new species (Pisces: Gobioidei). *Records of the Australian Museum, 36*, 169–201.

Risso, A. (1810). *Ichthyologie de Nice, ou histoire naturelle des poissons du Département des Alpes Maritimes*. Paris: F. Schoell.

Risso, A. (1827). *Histoire naturelle des principales productions de l'Europe méridionale et particulièrement de celles des environs de Nice et des Alpes Maritimes*. Paris & Strasbourg: F. G. Levrault.

Rocha, L. A., Robertson, D. R., Rocha, C. R., Van Tassell, J. L., Craig, M. T., & Bowens, B. W. (2005). Recent invasion of the tropical Atlantic by an Indo-Pacific coral reef fish. *Molecular Ecology, 14*(13), 3921–3928. https://doi.org/10.1111/j.1365-294X.2005.02698.x

Ronquist, F., Teslenko, M., van der Mark, P., Ayres, D. L., Darling, A., Höhna, S., Larget, B., Liu, L., Suchard, M. A., & Huelsenbeck, J. P. (2012). MrBayes 3.2: efficient Bayesian phylogenetic inference and model choice across a large model space. *Systematic Biology, 61*(3), 539–542. https://doi.org/10.1093/sysbio/sys029

Roşca, V. H. (2008). The modern interpretation of the Sarmatian basin history and its significance for stratigraphy. In P. F. Gozhik (Ed.), *Biostratigraphic fundamentals of creating the stratigraphic schemes of the Phanerozoic of Ukraine: Proceedings of the Institute of Geological Sciences of the NAS of Ukraine* (pp. 420–423). Kyiv.

Schneider, C. A., Rasband, W. S., & Eliceiri, K. W. (2012). NIH Image to ImageJ: 25 years of image analysis. *Nature Methods, 9*(7), 671–675. https://doi.org/10.1038/nmeth.2089

Schwarzhans, W. W. (2014). Otoliths from the middle Miocene (Serravallian) of the Karaman Basin Turkey. *Cainozoic Research, 14*(1), 35–69.

Schwarzhans, W., Agiadi, K., & Carnevale, G. (2020a). Late Miocene-Early Pliocene evolution of Mediterranean gobies and their environmental and biogeographic significance. *Rivista Italiana di Paleontologia e Stratigrafia, 126*(3), 657–724.

Schwarzhans, W., & Aguilera, O. A. (2024). Otoliths of the Gobiidae from the Neogene of tropical America. *Swiss Journal of Palaeontology, 143*(13), 1–129. https://doi.org/10.1186/s13358-023-00302-5

Schwarzhans, W., Ahnelt, H., Carnevale, G., Japundžić, S., Bradić, K., & Bratishko, A. (2017). Otoliths in situ from Sarmatian (Middle Miocene) fishes of the Paratethys. Part III: tales from the cradle of the Ponto-Caspian gobies. *Swiss Journal of Palaeontology, 136*(1), 45–92. https://doi.org/10.1007/s13358-016-0120-7

Schwarzhans, W., Brzobohatý, R., & Radwańska, U. (2020b). Goby otoliths from the Badenian (middle Miocene) of the Central Paratethys from the Czech Republic, Slovakia and Poland: A baseline for the evolution of the European Gobiidae (Gobiiformes; Teleostei). *Bollettino della Società Paleontologica Italiana, 59*(2), 125–173. https://doi.org/10.4435/bspi.2020.10

Schwarzhans, W., Klots, O., Kovalchuk, O., Dubikovska, A., Ryabokon, T., & Kovalenko, V. (2024). Life on a Miocene barrier reef - fish communities and environments in the Medobory backreef. *Palaeontologia Electronica*. https://doi.org/10.26879/1429

Schwarzhans, W., Klots, O., Ryabokon, T., & Kovalchuk, O. (2022). A rare window into a back-reef fish community from the middle Miocene (late Badenian) Medobory Hills barrier reef in western Ukraine, reconstructed mostly by means of otoliths. *Swiss Journal of Palaeontology*. https://doi.org/10.1186/s13358-022-00261-3

Smith, C. L. (1997). *Field guide to tropical marine fishes of the Caribbean, the Gulf of Mexico, Florida, the Bahamas, and Bermuda. National Audubon Society*. New York: Chanticleer Press Edition.

Steindachner, F. (1861). Beiträge zur Kenntniss der Gobioiden. *Sitzungsberichte der Kaiserlichen Akademie der Wissenschaften in Wien, mathematisch-naturwissenschaftliche Classe* 42 (23, Jahrgang 1860): 283–292.

Steindachner, F. (1870). Ichthyologische Notizen (X). (Schluss). *Sitzungsberichte der Kaiserlichen Akademie der Wissenschaften. Mathematisch-Naturwissenschaftliche Classe, 61*, 623–642.

Switchenska, A. A. (1973). Fossil mugiliforms of the USSR. *Trudy Paleontologiceskogo Instituta Akademii Nauk SSSR (In Russian), 138*, 1–64.

Teimori, A., Esmaeili, H. R., Gholami, Z., Zarei, N., & Reichenbacher, B. (2012). *Aphanius arakensis*, a new species of tooth-carp (Actinopterygii, Cyprinodontidae) from the endorheic Namak Lake basin in Iran. *Zookeys, 215*, 55–76. https://doi.org/10.3897/zookeys.215.1731

Thacker, C. E. (2015). Biogeography of goby lineages (Gobiiformes: Gobioidei): Origin, invasions and extinction throughout the Cenozoic. *Journal of Biogeography, 42*(9), 1615–1625. https://doi.org/10.1111/jbi.12545

Tornabene, L., Ahmadia, G. N., & Williams, J. T. (2013). Four new species of dwarfgobies (Teleostei: Gobiidae: *Eviota*) from the Austral, Gambier, Marquesas and Society Archipelagos, French Polynesia. *Systematics and Biodiversity, 11*(3), 363–380.

Vernerey, F. J., & Barthelat, F. (2014). Skin and scales of teleost fish: Simple structure but high performance and multiple functions. *Journal of the Mechanics and Physics of Solids, 68*, 66–76. https://doi.org/10.1016/j.jmps.2014.01.005

Vinciguerra, D. (1883). Risultati ittiologici delle crociere del Violante. *Annali del Museo Civico di Storia Naturale di Genova (Serie 3), 18*, 465–590.

Wang, H.-Y., Tsai, M.-P., Dean, J., & Lee, S.-C. (2001). Molecular phylogeny of gobioid fishes (Perciformes: Gobioidei) based on mitochondrial 12S rRNA sequences. *Molecular Phylogenetics and Evolution, 20*(3), 390–408. https://doi.org/10.1006/mpev.2001.0957

Wang, R., & Winterbottom, R. (2006). Osteology and phylogeny of *Parioglossus* (Teleostei, Gobioidei), with a revised key to the species. *Zootaxa, 1131*, 1–32.

Whitley, G. P. (1935). Studies in ichthyology. No. 9. *Records of the Australian Museum, 19*, 215–250.

Whitley, G. P. (1945). New sharks and fishes from western Australia. Part 2. *The Australian Zoologist, XI*, 1–42.

Winterbottom, R. (1993). Search for the gobioid sister group (Actinopterygii: Percomorpha). *Bulletin of Marine Science, 52*(1), 395–414.

Yakubovskaya, T.A. (1955). The Sarmatian flora of the Moldavian SSR. In B. K. Shishkin (Ed.) *Flora and systematics of higher plants*, 7–109. vol. 1. Moscow, Leningrad: Academy of Sciences of the USSR, Transactions of the Botanical Institute Ser. 1.

Zhu, D., Ortega, C. F., Motamedi, R., Szewciw, L., Vernerey, F., & Barthelat, F. (2012). Structure and mechanical performance of a "modern" fish scale. *Advanced Engineering Materials, 14*(4), B185–B194. https://doi.org/10.1002/adem.201180057